⌘ *Author's Choice*

Prion Protein-mediated Toxicity of Amyloid-β Oligomers Requires Lipid Rafts and the Transmembrane LRP1*

Jo V. Rushworth, Heledd H. Griffiths, Nicole T. Watt, and Nigel M. Hooper[1]

From the School of Molecular and Cellular Biology, Astbury Centre for Structural Molecular Biology, Faculty of Biological Sciences, University of Leeds, Leeds, LS2 9JT, United Kingdom

Background: Prion protein (PrP^C) is a receptor for amyloid-β oligomers (AβOs).
Results: AβO binding to PrP^C and cytotoxicity require transmembrane LRP1 and are reduced by cholesterol depletion and AβO remodeling.
Conclusion: Cellular binding and toxicity of AβOs are dependent on PrP^C being localized in a raft-based complex.
Significance: Remodeling AβOs and disrupting the prion-LRP1-raft interaction provide therapeutic targets for Alzheimer disease.

Soluble oligomers of the amyloid-β (Aβ) peptide cause neurotoxicity, synaptic dysfunction, and memory impairments that underlie Alzheimer disease (AD). The cellular prion protein (PrP^C) was recently identified as a high affinity neuronal receptor for Aβ oligomers. We report that fibrillar Aβ oligomers recognized by the OC antibody, which have been shown to correlate with the onset and severity of AD, bind preferentially to cells and neurons expressing PrP^C. The binding of Aβ oligomers to cell surface PrP^C, as well as their downstream activation of Fyn kinase, was dependent on the integrity of cholesterol-rich lipid rafts. In SH-SY5Y cells, fluorescence microscopy and co-localization with subcellular markers revealed that the Aβ oligomers co-internalized with PrP^C, accumulated in endosomes, and subsequently trafficked to lysosomes. The cell surface binding, internalization, and downstream toxicity of Aβ oligomers was dependent on the transmembrane low density lipoprotein receptor-related protein-1 (LRP1). The binding of Aβ oligomers to cell surface PrP^C impaired its ability to inhibit the activity of the β-secretase BACE1, which cleaves the amyloid precursor protein to produce Aβ. The green tea polyphenol (−)-epigallocatechin gallate and the red wine extract resveratrol both remodeled the fibrillar conformation of Aβ oligomers. The resulting nonfibrillar oligomers displayed significantly reduced binding to PrP^C-expressing cells and were no longer cytotoxic. These data indicate that soluble, fibrillar Aβ oligomers bind to PrP^C in a conformation-dependent manner and require the integrity of lipid rafts and the transmembrane LRP1 for their cytotoxicity, thus revealing potential targets to alleviate the neurotoxic properties of Aβ oligomers in AD.

Alzheimer disease (AD)[2] is a progressive and devastating neurodegenerative brain disorder from which over 37 million people are suffering worldwide (1) with an estimated cost of $600 billion in 2010 (2). The risk of developing AD correlates strongly with aging; therefore, AD is becoming an increasing socio-economic crisis as life expectancy increases. Despite this, there is no current therapy that can halt or reverse AD (3).

The key event driving AD pathogenesis is the accumulation of the 40–43-residue amyloid-β (Aβ) peptides in the brain (4). The peptides, particularly Aβ(1–42), are aggregation-prone, self-assembling to form a heterogeneous mixture of soluble oligomers, protofibrils, and fibrils. Soluble Aβ oligomers are found at elevated concentrations in AD brains, where their levels correlate strongly with AD onset and severity and are therefore proposed to be the major neurotoxic species in AD (5–7). Natural Aβ oligomers isolated from AD brains and cerebrospinal fluid, along with synthetic preparations and oligomers secreted by cultured cells, bind specifically to hippocampal neurons. Consequent deleterious effects include neurotoxicity, memory impairments, inhibition of long term potentiation, loss of dendritic spines, and synaptic dysfunction (7–10). The cellular mechanisms of Aβ oligomer-mediated neurotoxicity are, however, poorly defined.

Recently, the cellular prion protein (PrP^C) was identified as a high affinity receptor for Aβ oligomers (11). PrP^C is a glycosylphosphatidylinositol (GPI) anchored, cell surface glycoprotein that undergoes a conformational conversion to an infectious, protease-resistant form (PrP^{Sc}) in prion disorders such as Creutzfeldt-Jakob disease (12). PrP^C is, however, neuroprotective and plays important roles in neuronal oxidative stress defense and metal ion homeostasis in the brain (13). Aβ oligomers, but not monomers or fibrils, bound tightly to PrP^C ($K_d \approx 0.4$ nM) (11, 14), and the presence of PrP^C in hippocampal slices was shown to be responsible for the Aβ oligomer-mediated inhibition of long term potentiation (11). PrP^C was also

---

[2] The abbreviations used are: AD, Alzheimer disease; Aβ, amyloid-β; AFM, atomic force microscopy; APP, amyloid precursor protein; BACE1, β-site

APP cleaving enzyme-1; EGCG, (−)-epigallocatechin gallate; GPI, glycosylphosphatidylinositol; LDH, lactate dehydrogenase; LRP1, low density lipoprotein receptor-related protein-1; MβCD, methyl-β-cyclodextrin; PrP^C, cellular prion protein; RAP, receptor-associated protein; sAPPα, soluble ectodomain of APP from α-cleavage; sAPPβ, soluble ectodomain of APP from β-cleavage; SFKs, Src family kinase; AβO, amyloid-β oligomer; Tricine, N-[2-hydroxy-1,1-bis(hydroxymethyl)ethyl]glycine.

required for the manifestation of memory impairments in an AD mouse model (10), which were reversed by intracerebral infusion of an anti-PrP^C monoclonal antibody (15). Critically, immuno-targeting of PrP^C was shown to block completely the long term potentiation impairments caused by Aβ oligomers derived from human AD brain extracts (16, 17). Although the binding of Aβ oligomers to PrP^C has been confirmed by several groups (14, 18–21), whether PrP^C mediates the downstream Aβ oligomer neurotoxicity remains controversial (19, 20, 22).

Aβ is cleaved out of the amyloid precursor protein (APP) through the sequential action of the β-secretase BACE1 (β-site APP-cleaving enzyme-1) and the presenilin-containing γ-secretase complex (23). In the alternative nonamyloidogenic pathway, APP is first cleaved by the α-secretase, members of the ADAM (a disintegrin and metalloprotease) family of zinc metalloproteases, within the Aβ sequence thus precluding production of intact Aβ peptides. In both cell and animal models, PrP^C lowered Aβ production through the inhibition of BACE1, the rate-limiting enzyme in the generation of Aβ from APP (24, 25). On the basis of these data , we have previously proposed a model in which a normal function of PrP^C is to maintain a low level of Aβ through the inhibition of BACE1 (26).

Several different Aβ oligomers have been isolated from natural sources, such as AD brain extracts and cerebrospinal fluid, and also prepared synthetically from lyophilized peptide (27). These oligomers range in size from low *n* dimers and trimers to high molecular mass assemblies of over 1 MDa. Because of the heterogeneity in size and morphology of Aβ oligomers, the identification of the precise assemblies responsible for neurotoxicity in AD has proven difficult. The classification of oligomers according to their structural conformation can be considered a more biologically relevant parameter than size, as this provides information about the surface epitopes that may be important for binding to neuronal receptors (28). A panel of conformation-specific antibodies, generated by Glabe (28), indicates that oligomers can be classified into three categories based on the presentation of one of three mutually exclusive structural epitopes. The OC antibody recognizes the so-called fibrillar oligomers, which share a common structural epitope with fibrils, and may represent small fibril protofilaments (29). The A11 antibody recognizes pre-fibrillar oligomers that are early kinetic intermediates (30), and the α-annular protofibril antibody recognizes annular protofibrils or ring-shaped, pore-like oligomers (31). Of these three types of Aβ oligomers, only the fibrillar (OC-positive) oligomers were elevated significantly in human AD brain extracts and correlated with the onset and severity of AD (32).

The aim of this study was to determine whether PrP^C mediates the neuronal binding and toxicity of soluble, fibrillar OC-positive Aβ oligomers, which correlate with neuropathology in the AD brain, and to investigate the molecular and cellular mechanisms involved. We report that soluble, fibrillar OC-positive Aβ oligomers bind preferentially to, and display selective toxicity toward, cells and neurons expressing PrP^C. Disruption of lipid rafts through depletion of cholesterol reduces binding of the Aβ oligomers to the cells and blocks the downstream activation of a member of the Src family kinases (SFK), Fyn kinase. Aβ oligomers stimulate the endocytosis of cell surface

PrP^C in a mechanism dependent on the transmembrane low density lipoprotein receptor-related protein-1 (LRP1). LRP1 is also critical for the Aβ oligomer-mediated cytotoxicity. In addition, we show that the Aβ oligomers impair the PrP^C-mediated inhibition of BACE1, thus increasing the amyloidogenic processing of APP. Finally, using the polyphenolic compounds (−)-epigallocatechin gallate (EGCG) and resveratrol, which are known to remodel the conformation of Aβ oligomers (33–35), we show that conformation is a critical determinant of the binding of fibrillar Aβ oligomers to PrP^C.

EXPERIMENTAL PROCEDURES

Antibodies—SAF32 (anti-PrP N terminus) was from Cayman Chemical (Ann Arbor, MI); 6E10 (anti-Aβ(1–16)) and 3F4 (anti-PrP with the 3F4 epitope M108/M111) were purchased from Cambridge Bioscience Ltd. (Cambridge, UK); 6H4 (anti-PrP C terminus) was from Prionics AG (Switzerland); 22C11 (anti-APP) and anti-MAP2 were purchased from Millipore UK Ltd. (Livingston, UK); AC15 (anti-β-actin) was from Abcam (Cambridge, UK); anti-EEA1, anti-cleaved caspase-3 and anti-phospho-Src family kinase (Tyr-416) were from Cell Signaling Technology, Inc. (Danvers, MA); anti-cathepsin D was from Upstate Cell Signaling Solutions (Lake Placid, NY); anti-transferrin receptor was sourced from Invitrogen; anti-flotillin-1 was from BD Biosciences; and anti-LRP1 (N20) was from Santa Cruz Biotechnology. The conformation-specific antibodies OC and A11 were kind gifts from C. Glabe (University of California), and 1A9 (anti-sAPPβ) was provided by I. Hussain (GlaxoSmithKline, Harlow, UK). The fluorescently labeled secondary antibodies donkey anti-mouse and anti-goat AlexaFluor® 488 and 594 were from Molecular Probes, Inc. (Eugene, OR). Fluorescein isothiocyanate (FITC)- and Texas Red-conjugated streptavidin and goat anti-rabbit Cy5-IgG were purchased from Invitrogen.

Cell Lines and Culture—SH-SY5Y human neuroblastoma cells stably transfected with either empty pIRES*neo* (BD Biosciences) or expressing murine PrP^C containing the 3F4 epitope tag (human M108/M111) were prepared as described previously (36). In the pIRES vector the cDNA encoding PrP^C and the antibiotic resistance gene are translated from a single mRNA transcript, such that expression of the antibiotic resistance gene in the absence of PrP^C does not occur (37). Therefore, all cells that survive the selection process express PrP^C, which was confirmed by immunofluorescence microscopy with anti-PrP^C antibodies. Cells were routinely cultured in Dulbecco's modified Eagle's medium supplemented with 10% (v/v) fetal bovine serum (FBS). NB7 human neuroblastoma cells were cultured in RPMI 1640 medium (Sigma) supplemented with 10% (v/v) FBS. Cells were maintained in a humidified incubator at 37 °C in a 5% CO_2, 95% air atmosphere.

Preparation of Rat Primary Hippocampal Neurons—The hippocampi of 6–8-day-old Wistar rats were removed as described previously (38). Brain tissue was removed and incubated with 0.25 μg/ml trypsin for 15 min at 37 °C in phosphate-buffered saline (PBS). Trypsin digestion was terminated by the addition of equal amounts of PBS, supplemented with 16 μg/ml soybean trypsin inhibitor (type I-S; Sigma), 0.5 μg/ml DNase I (type II from bovine pancreas; 125 kilounits/ml; Sigma), and 1.5

mM $MgSO_4$. The tissue was then pelleted by centrifugation at $3000 \times g$ for 5 min, resuspended in 2 ml of PBS with 100 μg/ml soybean trypsin inhibitor, 0.5 μg/ml DNase I, and 1.5 mM $MgSO_4$, triturated gently, and then centrifuged at $3000 \times g$ for 5 min to pellet the hippocampal neurons. The pellet was resuspended in 5 ml of minimal Earle's medium supplemented with 10% (v/v) FBS, 13 mM glucose, 50 IU/ml penicillin, and 50 μg/ml streptomycin and added to poly-L-lysine (1.5 mg/ml)-coated coverslips (0.5 ml/well for 24-well plates). After 24 h, the medium was topped up to 1 ml. After a further 24 h, the culture medium was replaced with one containing 10% (v/v) heat-inactivated horse serum and 80 μM fluorodeoxyuridine to prevent proliferation of non-neuronal cells. After a further 24 h, the medium was replaced with serum-free Neurobasal medium, supplemented with 2% (v/v) B27, 50 IU/ml penicillin, 50 μg/ml streptomycin, 80 μM fluorodeoxyuridine, 25 mM glutamic acid, and 0.5 mM glutamine. All experiments were conducted on cells after 5–7 days in culture.

Aβ Oligomer Preparation—Synthetic biotin-Aβ(1–42) containing a 6-carbon linker between the biotin moiety and the N terminus of Aβ was purchased from AnaSpec (San Jose, CA). Aβ oligomers were prepared essentially as described previously (11, 39). Briefly, Aβ peptide was dissolved in 1,1,1,3,3,3,-hexafluoropropan-2-ol to break down any aggregated material, dried under a stream of N_2 gas, and stored at −80 °C. Peptide films of biotin-Aβ(1–42) were dissolved in dimethyl sulfoxide to 1 mM and then resuspended in Ham's F-12 medium (Lonza; Basel, Switzerland) to a final monomer concentration of 100 μM. Monomeric Aβ was taken at this point, whereas the remaining solution was incubated at room temperature for 16 h. The resulting preparation was centrifuged at $14,000 \times g$ for 20 min to pellet out any fibrillar material, and the supernatant was retained as the oligomer preparation. Pre-formed Aβ oligomers were incubated in the presence or absence of EGCG (4:1 molar excess) or resveratrol (10:1 molar excess) for 24 h at room temperature to remodel Aβ oligomers, and the resulting preparation was centrifuged at $14,000 \times g$ for 20 min to pellet out any fibrillar material (33–35).

Atomic Force Microscopy (AFM)—Samples were diluted in F-12 medium to ~500 nM peptide concentration and a 20-μl drop was placed onto a freshly cleaved mica film. Protein was allowed to adhere to the film for 90 s after which time the film was washed in distilled H_2O and dried under a stream of N_2 gas. Tapping mode AFM was performed using a Nanoscope IIIa Multimode-AFM instrument (Digital Instruments/Veeco; Phoenix, AZ) under ambient conditions. PointProbe®Plus AFM cantilevers (Windsor Scientific; Slough, UK) with a tip radius of <10 nm and resonance frequency of ~160 kHz were used. Fifty randomly selected particles were measured, and their volumes were calculated based on their shape being ellipsoid due to deposition on a surface ($V_{\text{ellipsoid}} = 4/3\pi \times r^2 \times$ height). The diameter of the sphere of corresponding volume was calculated for each particle, by rearranging the equation ($V_{\text{sphere}} = 4/3\pi \times r^3$) to give the diameter of the particle as it would exist in solution.

Flow Cytometry—SH-SY5Y cells were treated with Aβ oligomers at 4 °C to minimize internalization. Cells were then harvested in PBS containing EDTA, blocked with fish skin gelatin, incubated with FITC-streptavidin, and washed. Fluorescence was quantitated using a BD-LSRFortessa™ flow cytometer. Ten thousand events for each condition were measured, having gated the cell population to ensure that only live cells were monitored.

Dot Blotting—Samples were applied to dry nitrocellulose membrane (GE Healthcare). Membranes were blocked overnight in 10% (w/v) nonfat milk in the corresponding antibody diluent buffer (OC antibody (0.1 M Tris, 0.85% (w/v) NaCl, 0.1% (v/v) Triton X-100, pH 7.4), A11 antibody (20 mM Tris, 0.8% (w/v) NaCl, 0.001% (v/v) Tween 20, pH 7.4), or 6E10 antibody (0.1% (v/v) Tween 20 in PBS (PBST 1.5 mM NaH_2PO_4, 2.7 mM Na_2HPO_4, 150 mM NaCl, pH 7.4)). After washing, primary antibodies were applied for 1 h in the relevant buffer containing 3% (w/v) BSA (OC, 1:5000; A11, 1:1500; and 6E10, 1:4000). HRP-conjugated secondary antibodies were applied in the same buffer for 1 h. Bound HRP conjugates were visualized using the ECL® detection system (GE Healthcare). Semi-quantitative densitometry of dots was performed using ImageJ software (National Institutes of Health, Bethesda).

Western Blotting—Cell lysates were prepared routinely in lysis buffer (50 mM Tris, 150 mM NaCl, 0.5% (w/v) sodium deoxycholate, 1% (v/v) Nonidet P-40, pH 8.8). For phospho-SFK blots, cells were lysed in phosphatase inhibitor buffer (50 mM Tris, 150 mM NaCl, 1 mM sodium orthovanadate, 50 mM NaF, 0.4% (v/v) Nonidet P-40, 10% (v/v) glycerol, 10 μg/ml aprotinin, 20 μg/ml leupeptin, pH 7.5). Samples were mixed with dissociation buffer (100 mM Tris/HCl, 2% (w/v) SDS, 10% (v/v) glycerol, 100 mM DTT, 0.02% (w/v) bromphenol blue, pH 6.8). Cell lysate and conditioned media samples were boiled for 5 min. All proteins were resolved by SDS-PAGE on Tris-glycine acrylamide gels with the exception of Aβ oligomers that were resolved on Tris/Tricine 10–20% (v/v) acrylamide gradient gels (Bio-Rad) and then transferred to Hybond PVDF membranes (GE Healthcare). Following electrotransfer, the membranes were blocked for 1 h in PBST and 5% (w/v) nonfat milk. Membranes were incubated with primary antibody, either for 1 h at room temperature or overnight at 4 °C, followed by HRP-conjugated secondary antibody, both in PBST. Bound HRP conjugates were visualized using the ECL® detection system.

RNA Interference Studies—siRNA specific for human LRP1, human Fyn, and rat and human PrP^C, and a nontargeting sequence were obtained as smartpools from Dharmacon (Thermo Fisher Scientific Biosciences, Northumberland, UK). SH-SY5Y and NB7 cells were seeded into 6- or 24-well plates in routine culture medium and allowed to adhere overnight. The cell monolayers were washed twice with PBS containing Ca^{2+} and Mg^{2+} ions, and a 70 nM (final concentration) smartpool siRNA solution (Dharmacon) was delivered as a complex with DharmaFECT-1 (for SH-SY5Y and NB7 cells) or Dharma-FECT-3 (for rat primary hippocampal neurons) transfection reagent (Dharmacon) in serum-free medium. For LRP1, after 2 h, the serum-free medium was replaced with FBS-containing DMEM, and the cells were left for 25 h. For PrP^C and Fyn siRNA, the medium was left for 48 h prior to incubation of cells with Aβ oligomers and fixation for immunofluorescence microscopy or lysis for Western blot analysis.

Prion-mediated Toxicity of Aβ Oligomers

Methyl-β-cyclodextrin (MβCD) Treatment—SH-SY5Y cells expressing PrP^C or NB7 cells were incubated with 2 mM MβCD diluted in growth medium for 1 h at 37 °C. SH-SY5Y cells were incubated with oligomeric Aβ (200 nM total peptide) for 30 min on ice before visualization by fluorescence microscopy. NB7 cells were incubated with oligomeric Aβ (500 nM total peptide) for 20 min at 37 °C and lysates prepared as described above. NB7 lysates were assayed for cholesterol depletion using the Amplex Red cholesterol assay kit (Invitrogen) as described in the manufacturer's instructions.

Fluorescence Microscopy—Cells were cultured in normal growth medium to ~60% confluence on glass coverslips. For Aβ oligomer binding experiments, cells were incubated in the presence or absence of either monomeric Aβ or oligomers (200 nM total peptide concentration) diluted into F-12 medium (SH-SY5Y cells) or supplemented Neurobasal medium (primary neurons). To assess the effects of Aβ oligomers upon cell surface PrP^C, cells were incubated in the presence or absence of either Aβ oligomers (400 nM total peptide concentration) or 100 μM Cu^{2+} presented as a histidine chelate for 30 min at 37 °C. These experiments were conducted in the presence or absence of receptor-associated protein (RAP) at a concentration of 20 μg/ml. For LRP1 knockdown experiments, cells were incubated with Aβ oligomers (400 nM total peptide) for 30 min at 37 °C. For Aβ co-localization and internalization experiments, cells were incubated in the presence or absence of Aβ oligomers (400 nM total peptide concentration) at 37 °C for 1, 5, 20, 40, or 90 min. Postincubation, cells were fixed with 4% (v/v) paraformaldehyde or ice-cold 1:1 (v/v) methanol/acetone for 10 min, permeabilized if necessary using 0.2% (v/v) Tween 20 or 0.1% (v/v) Triton X-100 for 20 min (primary neurons), and blocked overnight at 4 °C in PBS containing Ca^{2+} and Mg^{2+} ions with 5% (v/v) fish skin gelatin. Coverslips were then incubated for 2 h in the same buffer containing primary antibody, washed, and then incubated with the appropriate fluorescent probe-conjugated secondary antibody under the same conditions. Nuclei were counterstained by washing briefly in DAPI stain, and coverslips were mounted onto glass slides using Fluoromount-G (Southern Biotech). Cells were visualized using a DeltaVision Optical Restoration Microscopy System (Applied Precision). Data were collected from at least 30 0.5-μm-thick optical sections, and three-dimensional data sets were deconvolved using the softWoRx program (Applied Precision). Images analyzed were individual *z*-sections taken from the middle of the data stack, representing a section through the center of the cell. The number of cells analyzed is indicated in individual figure legends. Fluorescence around the cell membrane was quantified using ImageJ software as described previously (40). This was plotted as pixel intensity *versus* distance around the cell using Microsoft Excel, and then the percentage of cell surface with detectable staining was calculated from multiple images. Bright field images were used to verify the location of the cell boundary.

Lipid Raft Isolation—Harvested cells were resuspended in 2 ml of MES-buffered saline (MBS: 25 mM MES, 150 mM NaCl, pH 6.5) containing 0.6% Triton X-100 and homogenized by passing 15 times through a Luer 21-gauge needle. The supernatant was made up to 40% sucrose by adding an equal volume of 80% sucrose in MBS. A 1-ml aliquot of the sample was placed below a discontinuous gradient of sucrose consisting of 3 ml of 35% sucrose and 1 ml of 5% sucrose, both in MBS. The samples were then centrifuged at 140,000 × *g* in an SW-55i rotor (Beckman Coulter) for 18 h at 4 °C. The sucrose gradients were harvested in 0.5-ml fractions from the base of the gradient, and the distribution of proteins was monitored by Western blot analysis of the individual fractions.

CytoTox-ONE^{TM} Homogeneous Membrane Integrity Assay—The assay kit (Promega), which measures the release of lactate dehydrogenase (LDH) from cells, was used in accordance with the manufacturer's instructions. Cells were plated out into black-walled 96-well plates and serum-starved overnight to synchronize the cells in the same phase of the cell cycle. Serum-containing medium was added for 2 h to re-start the cell cycle, before the cells were incubated with Aβ oligomers in Opti-MEM for 90 min at 37 °C. Lysis buffer was added to positive control wells. An equal volume of assay buffer was added to each well, and fluorescence was recorded at an excitation wavelength of 560 nm and an emission wavelength of 590 nm using a Varioskan Flash plate reader (Thermo Fisher Scientific, Waltham, MA).

Multi-Tox Fluor^{TM} Multiplex Cytotoxicity Assay—The assay kit (Promega) was used in accordance with the manufacturer's instructions. Cells were plated out as described for the LDH release assay. Aβ oligomers were added to the cells in Opti-MEM for 5 h at 37 °C, after which point an equal volume of assay buffer was added to each well, and the plate was incubated in the dark for at least 30 min at 37 °C. Fluorescence was recorded at an excitation of 400 nm and emission of 520 nm for live cell measurements and an excitation of 485 nm and emission of 520 nm for dead cell measurements, from which the ratio of live to dead cells was calculated for each condition.

Caspase-3 Assay—Cells were cultured to confluence, rinsed in PBS, and then incubated in serum-free Opti-MEM in the presence or absence of Aβ oligomers (500 nM total peptide). After 23 h, staurosporine (1 μM) was added for 30 min, and then lysates were prepared and subjected to Western blotting for cleaved (active) caspase-3.

Effect of Aβ Oligomers upon PrP^C-regulated BACE1 Activity—SH-SY5Y cells, expressing APP with either PrP^C or empty vector, were cultured to confluence and then washed in serum-free Opti-MEM. Cells were incubated in the presence or absence of Aβ oligomers (800 nM total peptide concentration) or heparin (800 nM) in serum-free Opti-MEM for 16 h at 37 °C. Conditioned medium was harvested and concentrated using Vivaspin 10-kDa molecular mass cutoff filters (Sartorius Stedim UK Ltd., Surrey, UK). Conditioned media and lysates were separated by SDS-PAGE and analyzed by Western blotting.

Statistical Analysis—Densitometric analysis was performed using ImageJ software. The nonparametric two-tailed Mann-Whitney *U* test was employed to compare two independent samples when sample numbers were less than *n* = 6. Where *n* > 6 and the data were normally distributed, as verified by the Kolmogorov-Smirnov test, the Levene test was used to ensure that the data sets were of equal variance. The parametric independent *t* test was subsequently used to calculate significance. *p* ≤ 0.05 was considered significant and error bars given
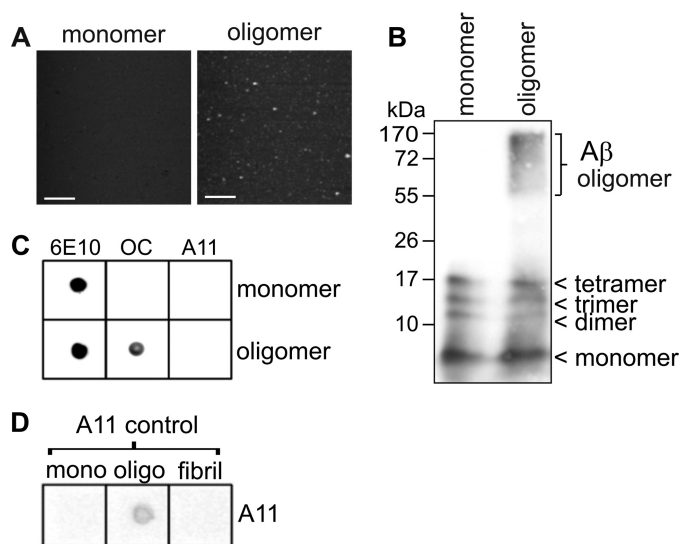
FIGURE 1. **Characterization of soluble, fibrillar Aβ oligomers.** Biotin-Aβ(1–42) oligomers were prepared as described under "Experimental Procedures". *A,* tapping mode AFM of freshly prepared Aβ monomer and oligomers (*scale bar,* 100 nm). *B,* freshly prepared Aβ monomers or oligomers were separated by denaturing Tris/Tricine SDS-polyacrylamide gel (2 μg of protein) and then immunoblotted and probed with the anti-Aβ antibody 6E10. *C,* samples of freshly prepared Aβ monomers and oligomers (1 μg of protein) were spotted onto nitrocellulose membrane and dot-blotted with the indicated antibodies. *D,* control samples of Aβ monomers, A11-positive oligomers, and fibrils were pre-dotted onto nitrocellulose membrane and subjected to dot-blotting using the A11 antibody.

as $\pm$ S.E. Data were analyzed using the PASW Statistics 17 program (Chicago).

RESULTS

Characterization of Soluble, Fibrillar Aβ Oligomers—We prepared soluble, fibrillar Aβ oligomers from synthetic biotin-tagged peptide as described previously (29). Characterization of the Aβ oligomer preparation by AFM revealed a homogeneous, fibril-free population of globular particles that were absent from the monomeric starting material (Fig. 1*A*). The majority of the particles corresponded to spheres with a diameter of 5–6 nm (data not shown). Biochemical analysis by Tris/Tricine SDS-PAGE and Western blotting revealed a broad band of high molecular mass ($\sim$55–170 kDa) Aβ species within the oligomer preparation that was absent from the monomer preparation (Fig. 1*B*). In both the oligomer and monomer preparations, species corresponding to dimer, trimer, and tetramer were also apparent (Fig. 1*B*), which are possibly an artifact of SDS-PAGE. Dot blotting with the conformation-specific antibodies OC (fibrillar epitope) and A11 (pre-fibrillar epitope) indicated that the Aβ oligomers displayed a fibrillar (OC-positive) conformation and did not react with the A11 antibody (Fig. 1*C*). A control preparation of A11-positive oligomers verified the reactivity of the A11 antibody (Fig. 1*D*).

PrP^C Mediates the Binding of Fibrillar Aβ Oligomers—The binding of Aβ oligomers to human SH-SY5Y neuroblastoma cells, which lack detectable levels of endogenous PrP^C, was compared with their binding to cells stably expressing PrP^C (Fig. 2*A*) (24, 36). Fluorescence microscopy revealed that the binding of the biotin-Aβ oligomers to cells expressing PrP^C was 10-fold higher compared with the binding to the untransfected

cells (Fig. 2, *B* and *C*). Furthermore, only minimal binding of monomeric Aβ to the cells expressing PrP^C was observed (Fig. 2, *B* and *C*). The selective binding of the Aβ oligomers to the cells expressing PrP^C was confirmed by flow cytometry (Fig. 2, *D* and *E*). Next, we examined the binding of fibrillar Aβ oligomers to rat primary hippocampal neurons following treatment with either siRNA against PrP^C or a nontargeting siRNA control (Fig. 2*F*). The specific siRNA reduced PrP^C in the neurons by 70.4% (Fig. 2*G*) and reduced Aβ oligomer binding by 59.4% (Fig. 2*H*). These data indicate that in both SH-SY5Y cells and primary neurons, PrP^C is the major binding site for fibrillar Aβ oligomers.

Fibrillar Aβ Oligomers Mediate Cytotoxicity and Activate Fyn in a PrP^C-dependent Manner—The cytotoxicity of the Aβ oligomers toward SH-SY5Y cells, either expressing PrP^C or containing empty vector, was determined by two different assays. The CytoTox-ONE^{TM} homogeneous membrane integrity assay (Promega) determines the extent to which the plasma membrane has been damaged by measuring the amount of LDH that is released from the cells. Incubation in the presence of Aβ oligomers caused an increase in LDH release from both cells expressing empty vector and those expressing PrP^C, with significantly greater membrane damage to the cells expressing PrP^C (Fig. 3*A*). The addition of lysis buffer to cells lacking or expressing PrP^C caused an increase in LDH release of 99.5 and 109.4% compared with control, respectively. The Multi-Tox Fluor^{TM} multiplex cytotoxicity assay (Promega) was employed to verify these results. Incubation in the presence of Aβ oligomers decreased the live/dead cell ratio in both cells expressing vector alone and in the PrP^C-expressing cells, with a significantly greater effect upon the cells expressing PrP^C (Fig. 3*B*). These data indicate that PrP^C is not simply a cell surface receptor for soluble, fibrillar Aβ oligomers but is also, at least in part, responsible for mediating their cytotoxic effects.

To determine the mechanism by which the Aβ oligomers promote cytotoxicity, activation of caspase-3 was investigated as Aβ oligomers have been reported to activate this pro-apoptotic enzyme (41, 42). In the absence of PrP^C, there was no significant difference in the amount of active, cleaved caspase-3 following addition of Aβ oligomers to the cells (Fig. 3, *C* and *D*). Although the Aβ oligomers caused an increase in the amount of active, cleaved caspase-3 in the cells expressing PrP^C (Fig. 3, *C* and *D*), this was mainly attributed to an up-regulation in the basal level of caspase-3 in the cells expressing PrP^C, as has been observed previously (43).

SFKs are involved in mediating the toxic effects of Aβ (44), and their activity can be modulated by PrP^C (45). The activation of SFKs can be monitored by measuring the expression of phospho-Tyr-416 using a phosphospecific antibody (pSFK416). We wanted to establish whether the binding of Aβ oligomers to PrP^C was required for the phosphorylation of SFKs in our system. For these experiments, we used NB7 neuroblastoma cells that endogenously express PrP^C (Fig. 3*E*). As with the primary neurons (Fig. 2, *F* and *H*), siRNA knockdown of PrP^C (89.4% reduction) caused a significant reduction (86.2%) in Aβ oligomer binding to the NB7 cells (data not shown). Incubation of the NB7 cells with Aβ oligomers caused a 37.3% increase in the amount of active, phosphorylated SFKs, when normalized to
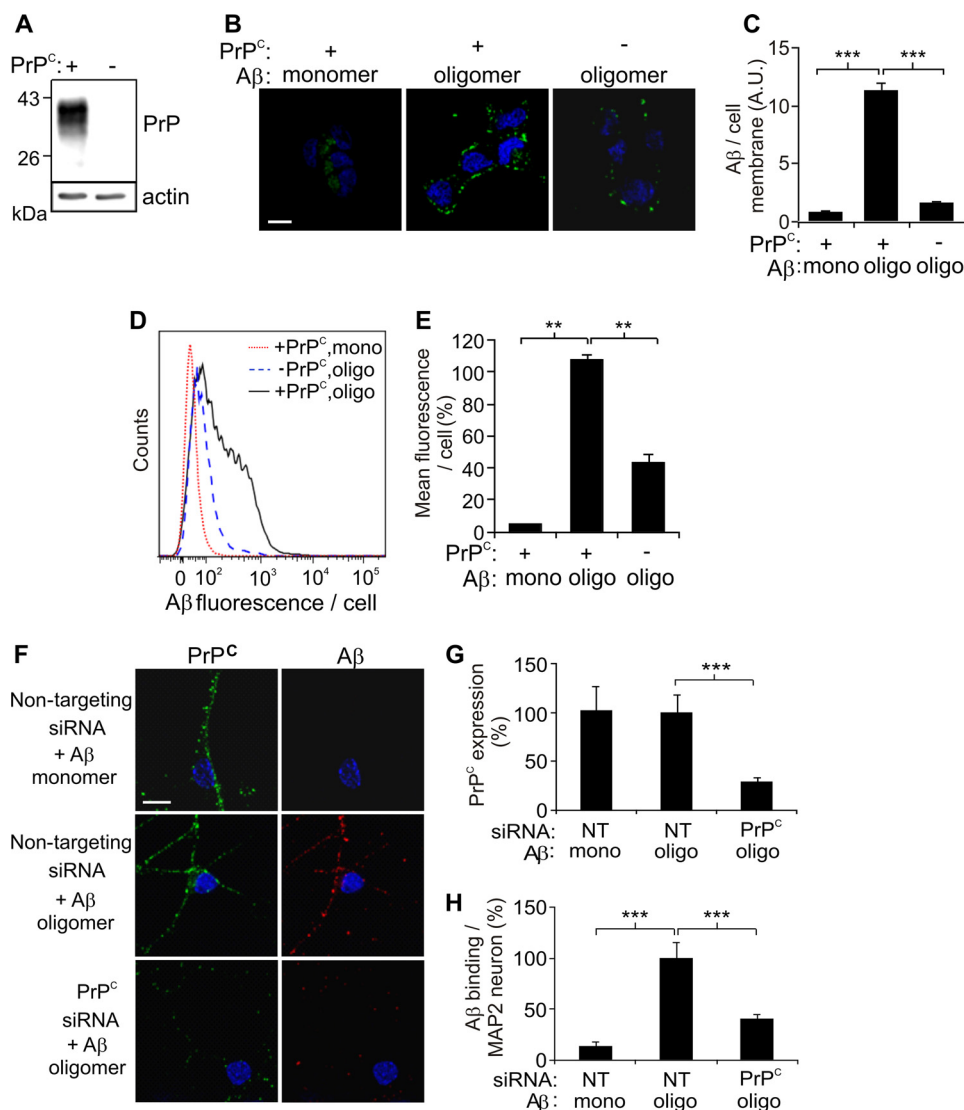
FIGURE 2. **PrP^C mediates the binding of Aβ oligomers to human neuroblastoma cells and rat hippocampal neurons.** *A,* Western blot of lysates (40 μg of protein) prepared from SH-SY5Y human neuroblastoma cells, either expressing PrP^C (+) or empty vector (−), with antibody 3F4 and for β-actin. *B,* SH-SY5Y cells, either expressing PrP^C (+) or empty vector (−), were incubated with fresh Aβ monomer or Aβ oligomers (200 nM total peptide) for 90 min at room temperature, washed, and then fixed onto slides. Biotin-Aβ oligomer/FITC-streptavidin conjugates (*green*) are observed as puncta around the cell membranes (*scale bar,* 5 μm). *C,* Aβ oligomer binding was quantified as the average fluorescence above threshold per length of cell boundary using ImageJ software (*n* = 60 for each condition; ***, *p* < 0.001; *A.U.,* arbitrary units). *D,* SH-SY5Y cells, stably expressing PrP^C (+) or empty vector (−), were incubated in the presence or absence of biotinylated Aβ monomer or oligomers (200 nM total peptide) for 30 min at 4 °C to minimize internalization. Cells were then harvested and incubated with FITC-streptavidin. Fluorescence per cell (corresponding to Aβ binding) was measured by flow cytometry. *E,* data were analyzed using FlowJo software (*n* = 3; **, *p* = 0.001). *F,* primary hippocampal neurons were isolated and grown for 5 days, then treated with siRNA targeted against PrP^C or a nontargeting (*NT*) control, and then incubated in the presence or absence of Aβ oligomer or monomer (200 nM total peptide) for 30 min at 4 °C. Cells were fixed, permeabilized, and then stained for Aβ oligomers and PrP^C using FITC-streptavidin and antibody 6H4, respectively (*scale bar,* 10 μm). The amount of PrP^C (*G*) and Aβ (*H*) per MAP2-positive neuron was quantified using ImageJ (*n* = 10; ***, *p* < 0.001).

total Fyn kinase levels (Fig. 3, *E* and *F*). Where the cells had been pretreated with the siRNA targeted against PrP^C, the addition of the Aβ oligomers did not lead to an increase in the amount of phosphorylated SFKs (Fig. 3, *E* and *F*). These data indicate that the activation of SFKs by Aβ oligomers is completely dependent on the presence of PrP^C. Although the phosphospecific antibody pSFK416 detects phospho-Tyr-416 in several SFKs, using kinase-specific immunoprecipitation, Um *et al.* (46) reported recently that the binding of Aβ oligomers to PrP^C specifically activates Fyn kinase. To confirm that the PrP^C-dependent activation was Fyn-specific, we used siRNA to knock down Fyn kinase that prevented the Aβ oligomer-mediated

activation of SFKs (Fig. 3, *G* and *H*), thereby confirming Fyn as the kinase activated upon binding of the Aβ oligomers to PrP^C.

Cholesterol Depletion Disrupts Aβ Oligomer Binding and Activation of Fyn—As both PrP^C and Fyn are localized to cholesterol-rich lipid raft domains (13, 47), we investigated whether the integrity of lipid rafts is required to mediate the binding of Aβ oligomers and the subsequent activation of Fyn. Treatment of the SH-SY5Y cells with MβCD caused re-distribution of the punctate cell surface pattern of raft-localized PrP^C to a more uniform staining typical of non-raft-localized proteins (Fig. 4, *A* and *B*), as reported previously (40). In addition, this treatment caused the re-localization of PrP^C and Fyn from
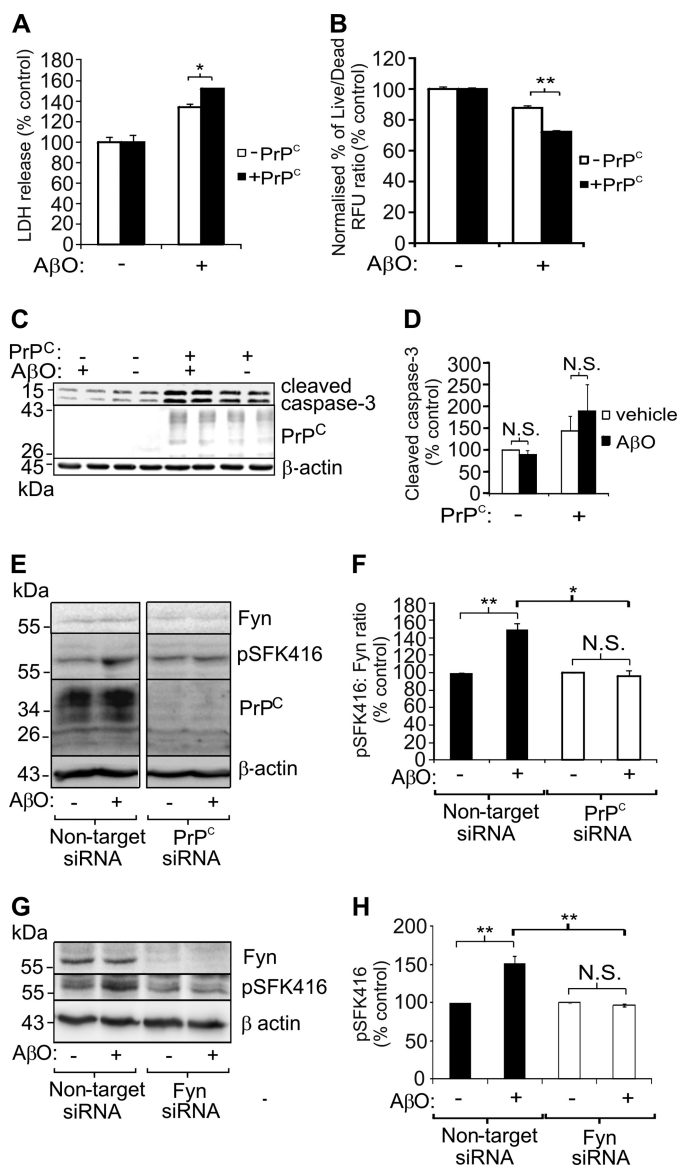
FIGURE 3. Aβ oligomers require the presence of PrP^C to mediate cytotoxicity and activation of Fyn kinase. *A,* cytotoxicity was measured using the CytoTox-ONE™ homogeneous membrane integrity assay. SH-SY5Y cells, expressing either PrP^C or empty vector, were incubated in the presence of either AβO (400 nM total peptide) or vehicle alone for 90 min at 37 °C ($n = 5$; *, $p = 0.016$). *B,* cytotoxicity was measured using the MultiTox-Fluor™ multiplex cytotoxicity assay. SH-SY5Y cells, expressing either PrP^C or empty vector, were incubated in the presence of either Aβ oligomers (400 nM total peptide) or vehicle alone for 5 h at 37 °C. Substrate was added, and fluorescence was measured to determine the ratio of live to dead cells for each condition, compared with control ($n = 5$; **, $p = 0.009$). *C,* SH-SY5Y cells expressing PrP^C (+) or empty vector (−) were incubated in Opti-MEM in the presence (+) or absence (−) of AβO (500 nM total peptide) for 23.5 h at 37 °C. Then staurosporine (1 μM) was added to the cells for 30 min. Cell lysates (100 μg of total protein) were immunoblotted for cleaved caspase-3 (anti-cleaved caspase-3, Asp-175), PrP^C (3F4), and β-actin. *D,* amount of cleaved caspase-3 was calculated from the immunoblots in *C* and normalized to β-actin (expressed as % control in the absence of Aβ oligomers) ($n = 4$; *N.S.,* not significant). NB7 cells were treated with nontargeting siRNA or siRNA against PrP^C (*E* and *F*) or Fyn (*G* and *H*) for 48 h, before incubating with Aβ oligomers (500 nM total peptide) (+) or vehicle control (−) for 20 min at 37 °C. Lysates were prepared and immunoblotted for Fyn, phospho-SFK (pSFK416), PrP^C (SAF32), and β-actin (*E*), and phospho-SFK, Fyn, and actin (*G*). The amount of phospho-SFK was calculated from the immunoblots in *F* and *H* normalized to Fyn kinase and presented as a percentage of the vehicle control, $n = 5$ (*E*), $n = 6$ (*G*); *, $p < 0.05$; **, $p < 0.01$; *N.S.,* not significant.

rafts to non-raft regions of the membrane (Fig. 4, *C* and *D*), consistent with the disruption of lipid rafts. Surprisingly, disruption of the rafts significantly reduced the cell surface binding of the Aβ oligomers (by 80.6%) (Fig. 4, *E* and *F*). In the NB7 cells, decreasing cholesterol levels by 32.7% (0 nM Aβ oligomers) and 40.9% (500 nM Aβ oligomers) (Fig. 4*G*) prevented the Aβ oligomers from activating Fyn kinase (Fig. 4, *H* and *I*). Together, these data indicate that lipid raft localization of PrP^C is required for the binding of Aβ oligomers and that the integrity of lipid rafts and/or other lipid raft-localized proteins are required for the Aβ oligomer-mediated activation of Fyn kinase.

On Binding to PrP^C, Aβ Oligomers Are Endocytosed and Trafficked to Lysosomes—Similar to the binding of other ligands to cell surface receptors, we hypothesized that following binding to PrP^C, the Aβ oligomers would be internalized along with their receptor. To investigate this, SH-SY5Y cells expressing PrP^C were incubated in the presence or absence of Aβ oligomers for 30 min at 37 °C. As a positive control, cells were incubated under the same conditions in the presence of 100 μM Cu^{2+}, presented as a histidine chelate, which stimulates PrP^C endocytosis (36). Incubation with either Cu^{2+} or Aβ oligomers caused a significant (40.1 and 59.0%, respectively) reduction in PrP^C at the cell surface (Fig. 5, *A* and *B*). We next explored the fate of the Aβ oligomers and PrP^C to determine whether they are internalized as a complex and to which subcellular compartments the Aβ oligomers are trafficked. Cells expressing PrP^C were incubated with Aβ oligomers at 37 °C over a time course from 1 to 90 min, prior to permeabilization and fixation. Fluorescence microscopy was used to assess the level of co-localization between Aβ oligomers and PrP^C and with organelle-specific markers (Fig. 5*C*). Quantitation of the amount of Aβ oligomers co-localized with PrP^C revealed a significant increase in their co-localization after 5 min, which increased up to 40 min and then diminished, albeit not significantly, after 90 min (Fig. 5*D*). This apparent increase in co-localization may be due to the Aβ oligomers and PrP^C aggregating together into larger complexes upon internalization. The co-localization of Aβ oligomers with EEA1, a marker for early endosomes, increased significantly between 1 and 5 min, continued to increase until 40 min, and then decreased significantly by 90 min (Fig. 5*E*). Co-localization of Aβ oligomers with a lysosomal marker, cathepsin D, showed a slight but significant increase after 40 min, with a more significant increase observed at 90 min (Fig. 5*F*). Taken together, these data indicate that Aβ oligomers, after binding to PrP^C at the cell surface, are internalized and trafficked to endosomes and then lysosomes.

Endocytosis and Cytotoxicity of Aβ Oligomers Are Dependent upon the Transmembrane LRP1—The Cu^{2+}-mediated internalization of PrP^C is dependent on the transmembrane LRP1 and can be blocked using the selective binding protein RAP (48, 49). We hypothesized, therefore, that LRP1 may play a role in the PrP^C-mediated binding, internalization, and cytotoxicity of Aβ oligomers. To investigate the involvement of LRP1 in the PrP^C-dependent binding and uptake of Aβ oligomers, siRNA was used to knock down the expression of LRP1 in the SH-SY5Y cells expressing PrP^C (Fig. 6, *A* and *B*). Targeted knockdown of LRP1 significantly reduced the cell surface binding (by 86.6%)
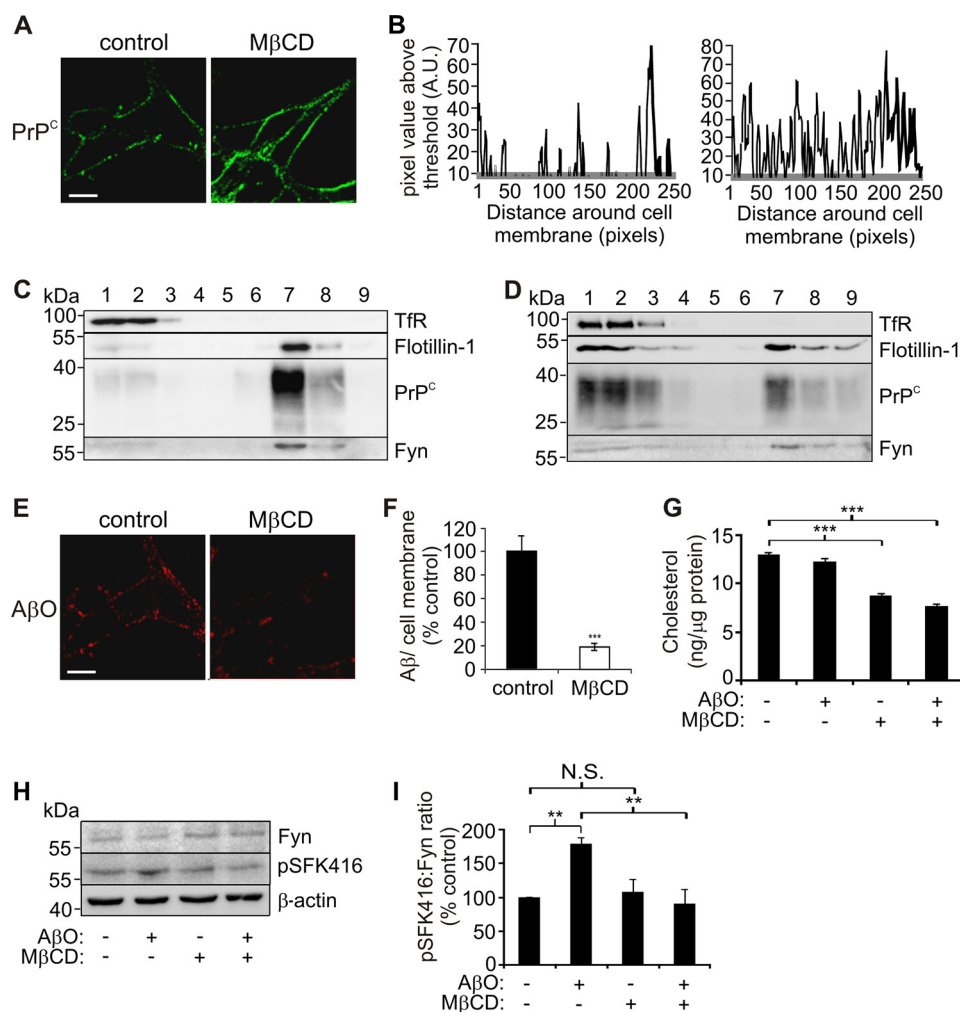
FIGURE 4. **Disruption of cholesterol-rich lipid rafts perturbs Aβ oligomer binding and activation of Fyn kinase.** SH-SY5Y cells expressing PrP^C were incubated in the absence (*control*) or presence of 2 mM MβCD for 1 h at 37 °C. Cells were then incubated with AβO (200 nM total peptide) for 30 min at 4 °C. *A*, cells were fixed and immunostained for PrP^C as described in Fig. 2 (*scale bar, 5 μm*). *B*, images presented in *A* were analyzed using ImageJ to determine the uniformity of PrP^C staining around the membrane in the presence or absence of MβCD (*A.U.*, arbitrary units). SH-SY5Y cells expressing PrP^C were incubated in the absence (*C*) or presence (*D*) of 2 mM MβCD for 1 h at 37 °C. Lipid rafts were prepared using a sucrose gradient and immunoblotted for transferrin receptor (*TfR*), Flotillin-1, PrP^C (3F4), and Fyn. Fractions labeled *1–9* with non-raft in fractions 1–3 and raft in fractions 7–9. Cells from *A* were also immunostained for Aβ (*E*), and the amount of Aβ per length of cell membrane was quantified using ImageJ (*n* = 10; ***, *p* < 0.001) (*F*). NB7 cells were incubated in the presence or absence of 2 mM MβCD for 1 h at 37 °C. Cells were then incubated with Aβ oligomers (*AβO +*, 500 nM total peptide) or vehicle (−) for 20 min at 37 °C. *G*, total cholesterol was measured in cell lysates using the Amplex Red cholesterol assay kit (*n* = 6; ***, *p* < 0.001). *H*, lysates were prepared and immunoblotted for Fyn, phospho-SFK (pSFK416), PrP^C, and β-actin. *I*, amount of phospho-SFK was calculated from the immunoblots in *H* normalized to Fyn kinase, and presented as a percentage of the vehicle control (*n* = 6; **, *p* < 0.01; *N.S.*, not significant).

of the Aβ oligomers (Fig. 6, *C* and *D*) and their internalization (by 77.8%) (Fig. 6, *E* and *F*). siRNA knockdown of LRP1 did not alter significantly the amount of PrP^C at the cell surface (Fig. 6*G*). A significant portion (90.5%) of the residual binding of Aβ oligomers to cells not expressing PrP^C was dependent on LRP1 (Fig. 6, *H–J*).

Next, we investigated the effect of Aβ oligomers upon the co-localization of PrP^C and LRP1 and whether the oligomers affected the trafficking of LRP1. Incubation of the SH-SY5Y cells with the Aβ oligomers caused a significant (50.2%) increase in the co-localization of PrP^C with LRP1 (Fig. 7, *A* and *B*). Incubation of the cells with the oligomers also significantly increased the co-localization of LRP1 with EEA1 after 10 min at 37 °C (Fig. 7, *C* and *D*). Together, these data suggest that LRP1 is a co-receptor that, along with PrP^C, mediates the binding and internalization of Aβ oligomers.

To investigate whether LRP1 is required for the cytotoxicity of Aβ oligomers, the LRP1-PrP^C interaction was inhibited by RAP (48). As RAP has been reported to bind monomeric Aβ (50), we initially investigated whether it would bind the fibrillar Aβ oligomers. Dot blotting revealed that the Aβ oligomers bound to recombinant PrP but did not interact with either RAP or BACE1 (Fig. 8*A*). Fluorescence microscopy revealed that in the presence of RAP, the binding of Aβ oligomers to SH-SY5Y cells expressing PrP^C was not altered (Fig. 8, *B* and *C*). However, RAP completely abolished the Aβ oligomer-dependent internalization of PrP^C (Fig. 8, *D* and *E*). When the cells were incubated with Aβ oligomers in the presence of RAP, there was no significant increase in LDH release, as observed in the cells treated with Aβ oligomers alone (Fig. 8*F*). To confirm that LRP1, and not another RAP-binding protein, was required for the toxicity of the Aβ oligomers, SH-SY5Y cells were incubated
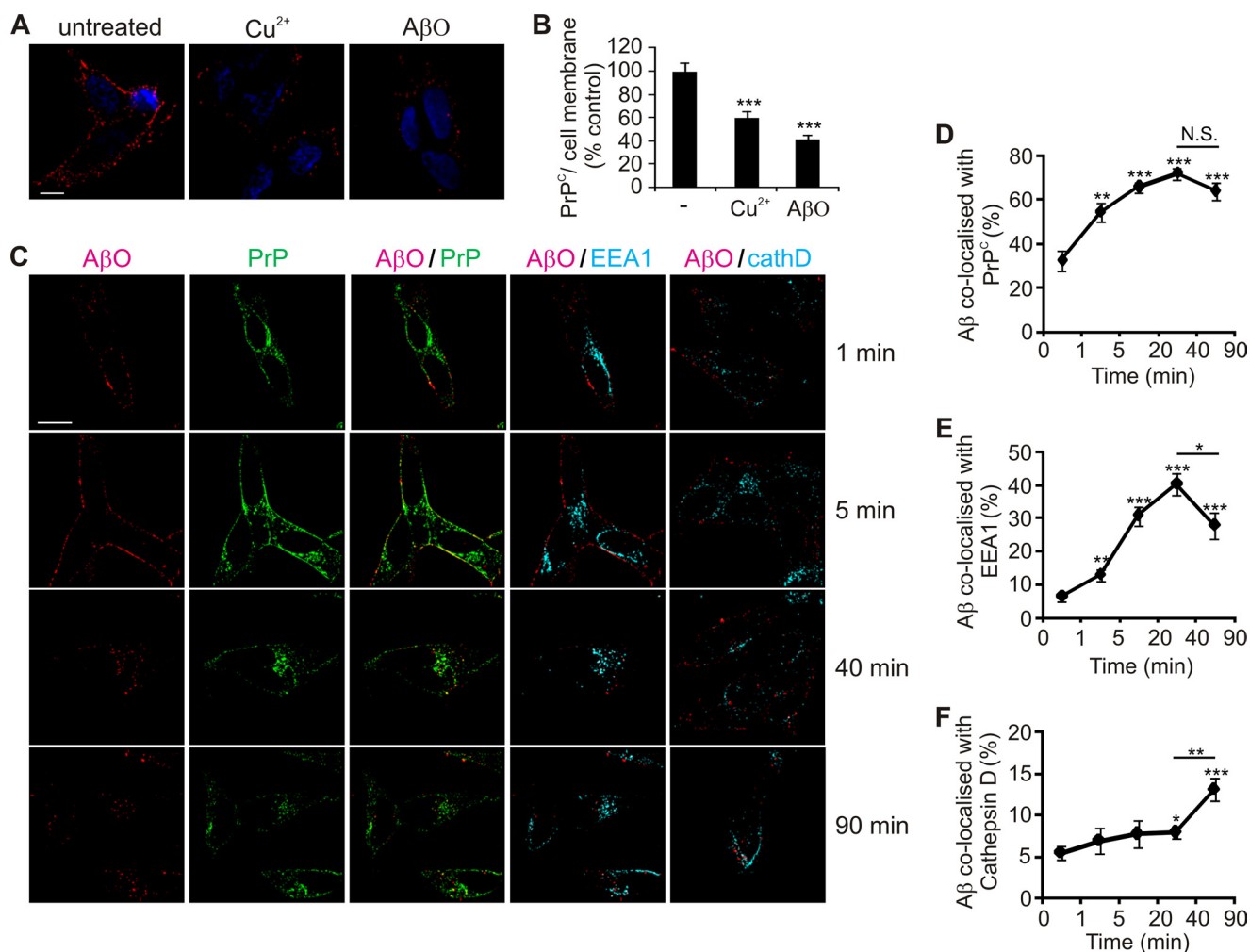
FIGURE 5. **Aβ oligomers endocytose with PrP^C and traffic to lysosomes.** *A,* SH-SY5Y cells expressing PrP^C were incubated for 30 min at 37 °C in the presence or absence of AβO (400 nM total peptide) or 100 μM Cu^{2+}. The cells were fixed and immunostained for PrP^C (SAF32) (*scale bar,* 5 μm). *B,* average fluorescence per length of cell membrane was quantified using ImageJ ($n = 20$ for each condition; ***, $p < 0.001$). *C,* SH-SY5Y cells expressing PrP^C were incubated with AβO (400 nM total peptide) at 37 °C for the times indicated before washing, fixation, and permeabilization. Aβ, PrP^C, endosomes, and lysosomes were detected using Texas Red-streptavidin, SAF32, anti-EEA1 and anti-cathepsin D, respectively (*scale bar,* 5 μm). Co-localization of Aβ oligomers with PrP^C (*D*), EEA1 (*E*), and cathepsin D (*F*) quantified using ImageJ ($n = 10$ for each condition; ***, $p < 0.001$; **, $p < 0.01$; *, $p < 0.05$; *N.S.,* not significant).

with Aβ oligomers in the presence of LRP1 siRNA. In the cells treated with the nontargeting siRNA, the Aβ oligomers caused a significant decrease in the live/dead cell ratio, although there was no such reduction in the live/dead cell ratio in the cells treated with the LRP1 siRNA (Fig. 8*G*). These data identify LRP1 as a novel co-receptor in the Aβ oligomer-PrP^C interaction, which is required for the PrP^C-mediated cytotoxicity of fibrillar Aβ oligomers.

Aβ Oligomers Impair the PrP^C-mediated Inhibition of BACE1—PrP^C interacts with the β-secretase BACE1 to prevent it from cleaving APP in the first step of Aβ generation, thus keeping Aβ monomer (and hence oligomer) levels to a minimum (24, 25). We hypothesized that Aβ oligomers, upon binding to PrP^C and promoting its internalization, may disrupt its inhibition of BACE1. To investigate this, initially we confirmed that PrP^C selectively inhibits the BACE1 cleavage of APP. In SH-SY5Y cells stably expressing APP along with either empty vector or PrP^C, there was a significant reduction (93.3%) in the amount of the BACE1 cleavage product (sAPPβ; soluble ecto-domain of APP from β-cleavage) but no effect on the α-secre-

tase cleavage product (sAPPα; soluble ectodomain of APP from α-cleavage) (Fig. 9*A*). Then cells were incubated in the presence or absence of Aβ oligomers. As a positive control, cells were also treated with heparin that increases the BACE1 cleavage of APP (24). Consistent with previous results (24), heparin stimulated the BACE1 cleavage of APP as evidenced by the increased amount of sAPPβ in the medium from both the cells expressing PrP^C (Fig. 9, *B* and *C*) and those lacking PrP^C (Fig. 9, *D* and *E*). In the SH-SY5Y cells expressing PrP^C, addition of the Aβ oligomers caused a significant increase in the amount of sAPPβ in the medium (Fig. 9, *B* and *C*). This effect was specific to the BACE1 cleavage of APP as the Aβ oligomers did not affect the amount of sAPPα (Fig. 9, *B* and *C*). In contrast, in the cells lacking PrP^C, the addition of Aβ oligomers had no effect on the amount of sAPPβ (Fig. 9, *D* and *E*). These data indicate that Aβ oligomers impair the ability of PrP^C to inhibit BACE1 activity, thus increasing the amyloidogenic processing of APP.

PrP^C-mediated Cellular Binding, Activation of Fyn, and Cyto-toxicity of Fibrillar Aβ Oligomers Are Conformation-dependent— Finally, we considered whether the fibrillar (OC-positive)
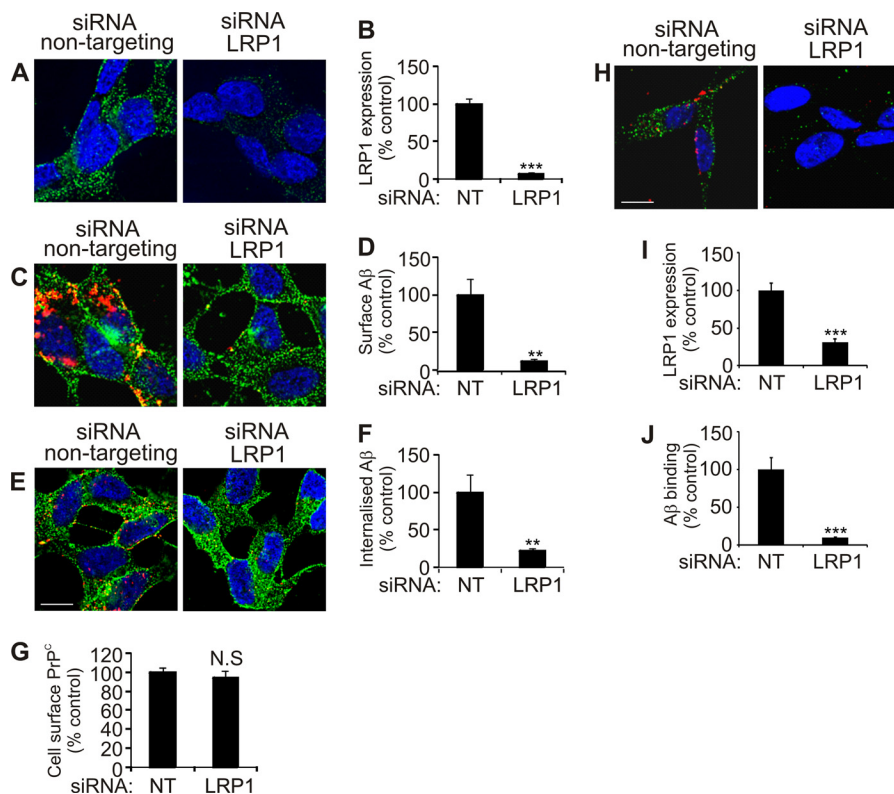
FIGURE 6. **Aβ oligomer binding and endocytosis of PrP^C are LRP1-dependent.** SH-SY5Y cells expressing PrP^C were incubated with either siRNA targeted against LRP1 or a nontargeting (*NT*) siRNA control. *A*, LRP1 was detected using anti-LRP1 (N20) antibody. *B*, LRP1 was quantified to verify the knockdown of protein expression ($n = 20$; ***, $p < 0.001$). Following siRNA treatment, cells were incubated with Aβ oligomers (400 nM total peptide) for 30 min and unpermeabilized to study Aβ oligomer binding (*C* and *D*) or permeabilized with Triton X-100 to study Aβ oligomer internalization (*E* and *F*). Aβ oligomers and PrP^C were detected using Texas Red-streptavidin and SAF32, respectively. Aβ oligomer binding (*D*), internalization (*F*), and cell surface levels of PrP^C (*G*) were quantified using ImageJ ($n = 10$; **, $p < 0.01$; $n = 20$; *N.S.*, not significant). *H*, SH-SY5Y cells expressing empty vector were incubated with either siRNA targeted against LRP1 or a nontargeting (*NT*) siRNA control. Following siRNA treatment, cells were incubated with Aβ oligomers (400 nM total peptide) for 30 min. LRP1 and Aβ oligomers were detected as described above, and LRP1 knockdown (*I*) and Aβ oligomer binding (*J*) were quantified using ImageJ ($n = 10$; ***, $p < 0.001$).

epitope may be a crucial structural motif that facilitates the interaction between Aβ oligomers and PrP^C. For this, we investigated whether EGCG and resveratrol (Fig. 10*A*), which have previously been shown to remodel Aβ oligomers (34, 35), could also remodel the fibrillar Aβ oligomers, disrupt their binding to PrP^C, and their PrP^C-mediated cytotoxicity. Tapping mode AFM revealed that EGCG and resveratrol both altered the morphology of the Aβ oligomers, causing them to be more diffuse and amorphous in shape and more heterogeneous in size (Fig. 10*B*). Dot-blotting showed that treatment with EGCG or resveratrol caused a significant reduction in OC immunoreactivity (82.9 and 66.4%, respectively) without significant alteration in 6E10 binding (Fig. 10, *C* and *D*).

Samples of the EGCG- and resveratrol-treated Aβ oligomers were incubated with SH-SY5Y cells expressing PrP^C, and cellular binding was determined. Fluorescence microscopy revealed that Aβ oligomers that had been treated with either EGCG or resveratrol displayed significantly reduced binding to the PrP^C-expressing cells (50.8 and 54.8%, respectively) (Fig. 10, *E* and *F*). As EGCG, albeit at a higher concentration (50 μM and upwards) than used in our experiments, has been reported to promote the internalization of PrP^C (51), SH-SY5Y cells expressing PrP^C were incubated with EGCG or resveratrol in the absence of Aβ oligomers. Fluorescence microscopy revealed that neither EGCG nor resveratrol caused a reduction

in the amount of PrP^C at the cell surface under these conditions (data not shown).

Next, we considered whether remodeling the oligomers would also disrupt the PrP^C-mediated activation of Fyn kinase. Treatment of the oligomers with either EGCG or resveratrol prevented the Aβ oligomer-mediated activation of Fyn in the NB7 cells (Fig. 10, *G* and *H*). Finally, the cytotoxicity of the EGCG- and resveratrol-remodeled Aβ oligomers toward SH-SY5Y cells expressing PrP^C was determined using the Multi-Tox Fluor^{TM} multiplex cytotoxicity assay. Treatment of the oligomers with either EGCG or resveratrol prevented the Aβ oligomer-mediated decrease in the live/dead cell ratio (Fig. 10*I*). Together these data indicate that EGCG and resveratrol remodel soluble, fibrillar Aβ oligomers into a distinct nonfibrillar conformation that has a reduced propensity to bind to PrP^C-expressing cells, is nontoxic, and is no longer able to activate Fyn.

DISCUSSION

Recent studies have identified PrP^C as a critical modulator of the AD-related synaptic dysfunction and cognitive impairments caused by Aβ oligomers (11, 17, 21, 42). Here, we reveal details of the molecular and cellular mechanisms underpinning the PrP^C-Aβ oligomer interaction and the resulting downstream cellular events. Our data indicate that the integrity of
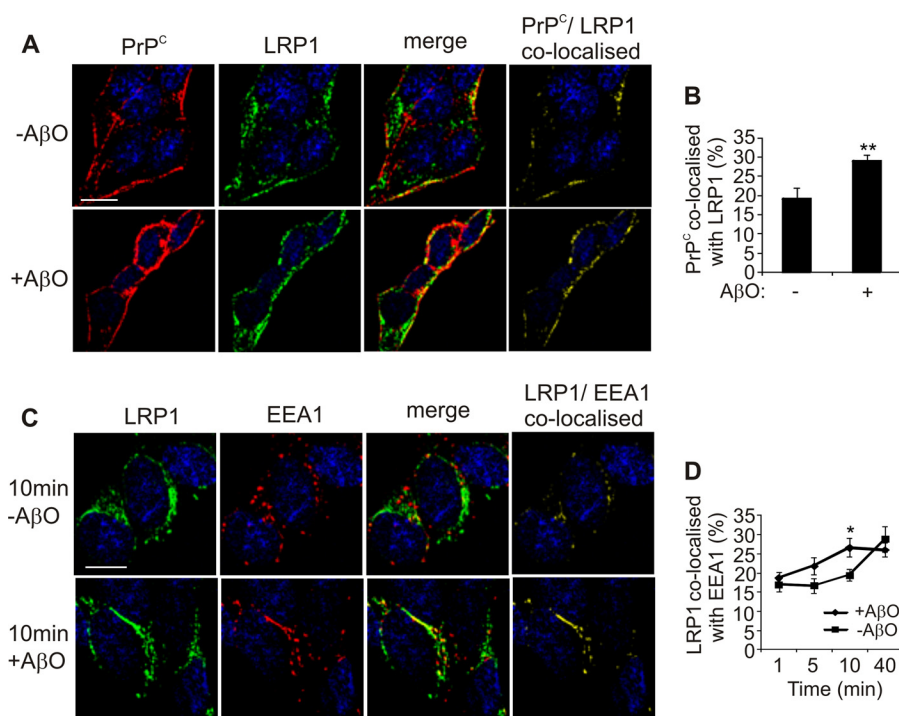
FIGURE 7. **Aβ oligomers promote the co-localization of PrP^C with LRP1 and increase the rate of LRP1 endocytosis.** *A,* SH-SY5Y cells expressing PrP^C were incubated in the presence or absence of AβO (400 nM total peptide) for 30 min at 4 °C. Cells were washed, fixed, and immunostained for PrP^C and LRP1 using the antibodies SAF32 and N20, respectively. *B,* amount of PrP^C co-localized with LRP1 was quantified in ImageJ (*n* = 10; **, *p* = 0.006). *C,* SH-SY5Y cells expressing PrP^C were pre-labeled with anti-LRP1 antibody (N20) at 4 °C for 30 min and then washed to remove unbound antibody. Cells were transferred to 37 °C and incubated with medium in the presence or absence of AβO (400 nM total peptide) for 1, 5, 10, or 40 min prior to washing, fixation, and permeabilization in 0.2% Tween 20 and stained for early endosomes (anti-EEA1) along with LRP1. Only images for the 10-min time point are shown. *D,* percentage of total LRP1 that was co-localized with EEA1 was quantified in ImageJ (*n* = 15; *, *p* = 0.016). *Scale bars,* 5 μm.

cholesterol-rich lipid rafts is critical for both the interaction of fibrillar Aβ oligomers with PrP^C and to mediate the activation of downstream Fyn kinase. We show that the PrP^C-mediated binding and cytotoxicity of Aβ oligomers is dependent upon the transmembrane LRP1. We also reveal that Aβ oligomers disrupt the PrP^C-mediated inhibition of BACE1 that normally dampens amyloidogenic processing. Finally, we show that disrupting the conformation of Aβ oligomers can prevent their PrP^C-dependent binding and toxicity.

The conformation of Aβ oligomers is a key determinant of their biological functions (28, 33). Because Aβ oligomers are heterogeneous in size and morphology, understanding the relationship between PrP^C binding, cytotoxicity, and Aβ oligomer conformation is paramount. In a recent study, only levels of the soluble, fibrillar (OC-positive) oligomers were found to be elevated significantly in AD brains, where they correlated strongly with AD severity and the stage of the disease (32). Interestingly, these fibrillar Aβ oligomers were found at particularly high levels in regions of the brain (hippocampus, cortex, and olfactory bulb) that also have high physiological PrP^C expression (52, 53). Therefore, we prepared fibrillar, OC-positive Aβ oligomers and characterized them both biophysically and through the use of conformation-dependent antibodies, prior to studying their binding to PrP^C. These fibrillar, OC-positive Aβ oligomers bound to both neuroblastoma cells and primary neurons in a PrP^C-dependent manner. In addition, PrP^C was required for the downstream cytotoxicity of the fibrillar Aβ oligomers and the activation of Fyn kinase. Fyn kinase is an SFK that is implicated in multiple pathways that underlie AD (54), including

mediating the toxicity of Aβ oligomers (44) and linking Aβ to Tau toxicity (55). While this work was under review, Um *et al.* (46) reported that the binding of Aβ oligomers to PrP^C activates Fyn and that activation of Fyn was required for *N*-methyl-D-aspartate receptor phosphorylation and cell surface distribution, dendritic spine loss, and LDH release.

The GPI-anchored PrP^C is localized to cholesterol-rich lipid raft microdomains of the plasma membrane (13). Cholesterol depletion disrupts these rafts with PrP^C being redistributed into non-raft regions of the membrane (40). Interestingly, we found that disruption of the rafts caused a significant (80%) reduction in Aβ oligomer binding to the cells and prevented the activation of the Fyn kinase. The intracellular signaling from PrP^C is known to be dependent on the integrity of lipid rafts (56), and our data clearly indicate that not only the downstream signaling mechanisms but also the binding of the oligomers to PrP^C is dependent on the integrity of the raft microdomains. This would also be consistent with the observation that toxic signaling of Aβ oligomers via PrP^C requires its GPI anchorage (21).

Other ligands such as Cu^{2+} (40) and stress-inducible protein 1 (57) promote the endocytosis of PrP^C. Thus we hypothesized that Aβ oligomers would also promote the endocytosis of PrP^C. Indeed, the Aβ oligomers co-internalized with PrP^C from the cell surface and then trafficked to endosomes and lysosomes. A previous study showed that Aβ oligomers are taken up by endocytosis and traffic to endosomes and lysosomes and that blocking their internalization ablates toxicity (58). In contrast to our data, a recent study found that Aβ oligomers caused a rapid
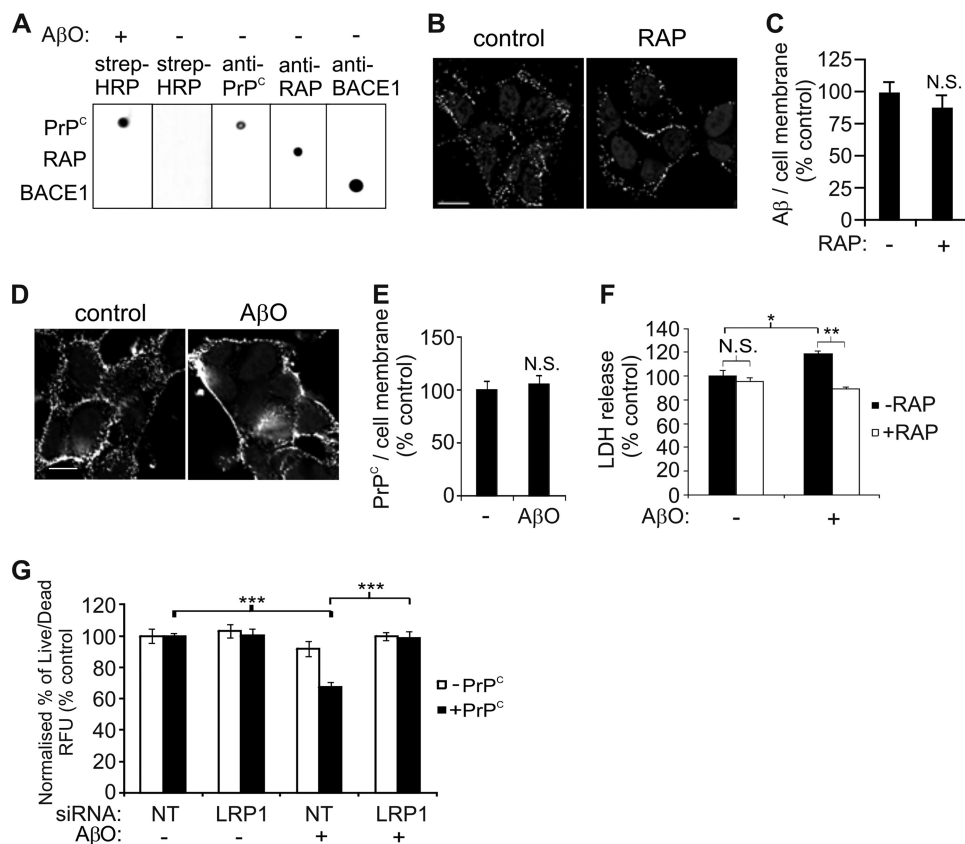
FIGURE 8. **Disruption of the PrP^C-LRP1 interaction blocks Aβ oligomer-mediated PrP^C internalization and toxicity.** *A,* recombinant human PrP, recombinant human RAP, and recombinant human BACE1 (1 μg of each) were spotted onto nitrocellulose membranes and blocked in 10% milk for 1 h. The membrane was incubated in the presence or absence of biotin-AβO (250 nM diluted in PBS) for 1 h, prior to probing with streptavidin-conjugated horseradish peroxidase (*strep-HRP*). Replicate membranes were probed to verify the presence of PrP^C (SAF32), RAP (anti-RAP), and BACE1 (EE17). *B,* SH-SY5Y cells expressing PrP^C were incubated in the presence or absence of RAP (20 μg/ml) for 10 min prior to incubation with Aβ oligomers (400 nM total peptide) for 30 min at room temperature. Following washing and fixation, Aβ oligomers were detected using Texas Red-conjugated streptavidin (*scale bar,* 5 μm). *C,* average fluorescence per length of cell membrane was quantified using ImageJ (*n* = 10; *N.S.,* not significant). *D,* SH-SY5Y cells expressing PrP^C were incubated for 30 min at 37 °C in the presence or absence of AβO (400 nM total peptide) along with RAP (20 μg/ml). The cells were fixed and immunostained for PrP^C (*scale bar,* 5 μm). *E,* average fluorescence per length of cell membrane was quantified using ImageJ (*n* = 20 for each condition; *N.S.,* not significant). *F,* cytotoxicity was measured using the CytoTox-ONE^{TM} homogeneous membrane integrity assay. SH-SY5Y cells expressing PrP^C were pre-incubated in the presence or absence of RAP (20 μg/ml) for 60 min in serum-free Opti-MEM and then incubated for a further 90 min with either AβO (400 nM total peptide) or vehicle alone for 90 min at 37 °C (*n* = 5; *,* p = 0.028; **, p = 0.009; *N.S.,* not significant). *G,* cytotoxicity was measured using the MultiTox-Fluor^{TM} multiplex cytotoxicity assay. SH-SY5Y cells, expressing either PrP^C or empty vector, were incubated with either siRNA targeted against LRP1 or a nontargeting (*NT*) siRNA control, and then incubated in the presence of either Aβ oligomers (400 nM total peptide) or vehicle alone for 5 h at 37 °C. Substrate was added, and fluorescence was measured to determine the ratio of live to dead cells for each condition, compared with control (*n* = 5; ***, p < 0.001).

increase in cell surface PrP^C and inhibited its endocytosis (59). However, the Aβ oligomers used by Caetano *et al.* (59) were not characterized either biophysically or immunologically and were used at a significantly higher concentration. The trafficking of PrP^C has been shown to occur via multiple mechanisms that can vary between cell types (56), and it is possible that different Aβ oligomer preparations may have differential effects on these systems.

Critically, we reveal that the PrP^C-mediated binding, toxicity, and subsequent internalization of Aβ oligomers are dependent upon LRP1. LRP1 is one of the largest members of the low density lipoprotein receptor family and is highly expressed in neuronal cells (60). LRP1 is a transmembrane protein that facilitates the clathrin-mediated endocytosis of PrP^C (48) and that has previously been implicated in the neuronal uptake of Aβ oligomers (61, 62). Although LRP1 resides largely in non-raft regions of the plasma membrane, it is known to interact transiently with lipid rafts (63). Our data indicate that LRP1 functions as a transmembrane co-receptor that is involved in the Aβ oligomer-PrP^C interaction and is required for their internalization. Because the first observation that the GPI-anchored PrP^C was a receptor for Aβ oligomers (11), it has been postulated that there is a transmembrane co-receptor required to connect the binding of the oligomers on the outer surface of the plasma membrane with downstream effects inside the cell (64). However, the identity of such a transmembrane co-receptor has remained elusive. Our observation that LRP1 is required for both the internalization and cytotoxicity of the Aβ oligomers indicates that LRP1 is a likely candidate for such a transmembrane co-receptor.

Emerging evidence suggests that PrP^C interacts with other membrane proteins to generate lipid raft-based signaling complexes (65). An antibody blocking approach was used to demonstrate that Aβ oligomers co-localize with PrP^C, mGluR5, and *N*-methyl-D-aspartate receptors at the synapse (66). Upon binding, the Aβ oligomers promoted the clustering of the cell surface proteins and decreased their lateral movement in the membrane. Here, we show that Aβ oligomers also promote the
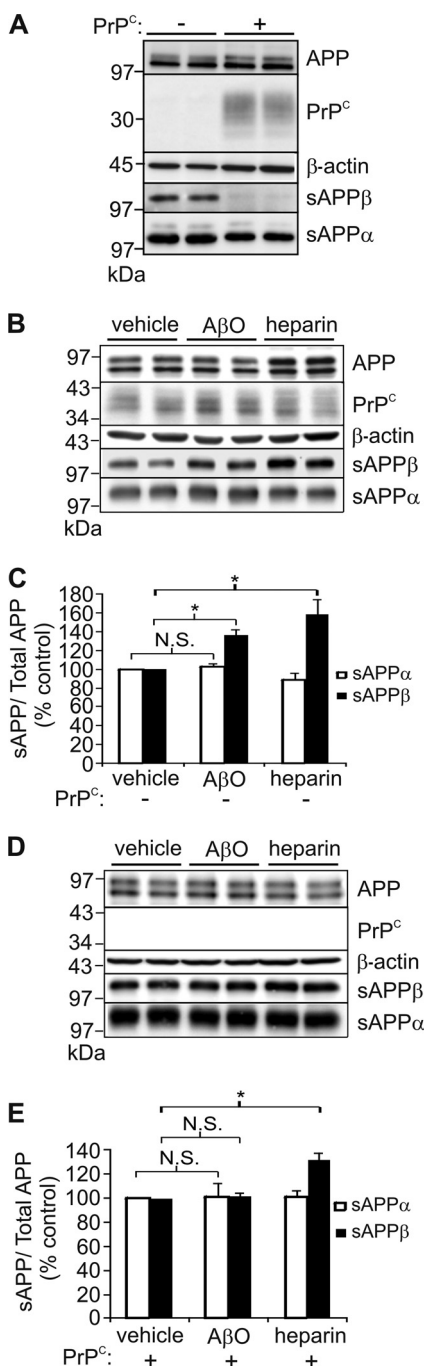
FIGURE 9. **Aβ oligomers impair the PrP^C-mediated inhibition of BACE1.** SH-SY5Y cells expressing APP$_{695}$ along with either PrP^C (+) or empty vector (−) were cultured to confluence and incubated in the presence of vehicle alone, AβO (800 nM total peptide), or heparin (800 nM). *A,* cell lysates and conditioned media immunoblotted (40 μg of protein) for APP (22C11), sAPPα (6E10), sAPPβ (1A9), PrP^C (3F4), and β-actin. Samples from cells expressing (*B* and *C*) or lacking (*D* and *E*) PrP^C were blotted as described above, and semi-quantitative densitometry of membranes was performed in ImageJ. Levels of sAPPα and sAPPβ were normalized to total APP ($n = 3$; *, $p < 0.05$). *N.S.,* not significant.

clustering of PrP^C with LRP1. These data suggest that Aβ oligomers induce the formation of a lipid raft-based multiprotein receptor complex that is critical to the binding, toxicity, and metabolism of the oligomers and that PrP^C and LRP1 are key structural and functional components of this signaling complex (Fig. 11). The small molecule RAP blocks the interaction of

LRP1 with its ligands, including PrP^C. However, the fact that RAP does not block the binding of Aβ oligomers to cells suggests that the majority of the Aβ oligomers do not bind directly to LRP1 but rather to another component (PrP^C) in the raft-based multiprotein receptor complex. It is the interaction between LRP1 and PrP^C that is disrupted by RAP and blocks the downstream cytotoxicity and internalization of the oligomers.

Previously, LRP1 has been reported to mediate the neuronal uptake of monomeric Aβ(1–42) (61, 62), and a recent study revealed that PrP^C mediates the transcytosis of monomeric Aβ(1–40) across the blood-brain barrier (67). PrP^C bound Aβ(1–40) in the low picomolar range, and both PrP^C knockdown and anti-PrP^C antibodies reduced significantly Aβ clearance in a blood-brain barrier model (67). Although PrP^C was found to co-immunoprecipitate with LRP1, RAP treatment did not affect the PrP^C-mediated transcytosis of Aβ (67). Although these earlier studies used monomeric preparations of Aβ, while we focused on the neurotoxic oligomeric form, these findings corroborate our data identifying LRP1 as an important co-factor in the PrP^C-mediated binding of Aβ.

The ability of Aβ oligomers to stimulate the endocytosis of PrP^C, thus lowering its cell surface expression, raised the possibility of secondary effects on the physiological functions of cell surface PrP^C. We have reported previously that PrP^C negatively regulates Aβ production through the inhibition of the β-secretase, BACE1, in part through an interaction at the cell surface that is dependent on glycosaminoglycans (24). Therefore, we explored whether the binding of the Aβ oligomers to PrP^C and their subsequent internalization would disrupt the PrP^C-mediated inhibition of BACE1. The fibrillar Aβ oligomers impaired the ability of PrP^C to inhibit BACE1, thus increasing the amyloidogenic processing of APP. These data agree with the model that we proposed previously whereby, in AD, Aβ oligomers bind to PrP^C and disrupt its ability to inhibit BACE1, in turn increasing Aβ levels (26). Thus, in the AD state, PrP^C is no longer protective but contributes to Aβ oligomer neurotoxicity and further Aβ production in a toxic, positive feedback loop. Interestingly, the interaction of PrP^C with BACE1 (24) and the interaction of PrP^C with LRP1 (40, 48) are both dependent upon the polybasic N-terminal sequence (KKRP) of PrP^C. This same region has recently been identified as a crucial determinant of PrP^C-mediated Aβ oligomer binding and toxicity. Surface plasmon resonance studies showed that deletion of the N-terminal first five residues of PrP^C caused a significant (∼8-fold) reduction in Aβ oligomer binding (14), and the deletion of the N terminus blocked the toxicity of synthetic and natural Aβ oligomers (21). Thus, this region appears to be critical to a number of functions of PrP^C, although its role in protective functions (24, 38, 68, 69) raises questions as to whether targeting the interaction of this region with Aβ oligomers would be a viable approach for the treatment of AD.

To explore the importance of the conformation of the Aβ oligomers in the PrP^C-mediated binding and cytotoxicity, we used EGCG and resveratrol to remodel the fibrillar epitope. Although both of these compounds have been shown previously to remodel prefibrillar oligomers (34, 35), only resveratrol has been reported to remodel soluble, fibrillar oligomers (34). The remodeled, nonfibrillar Aβ oligomers displayed signifi-
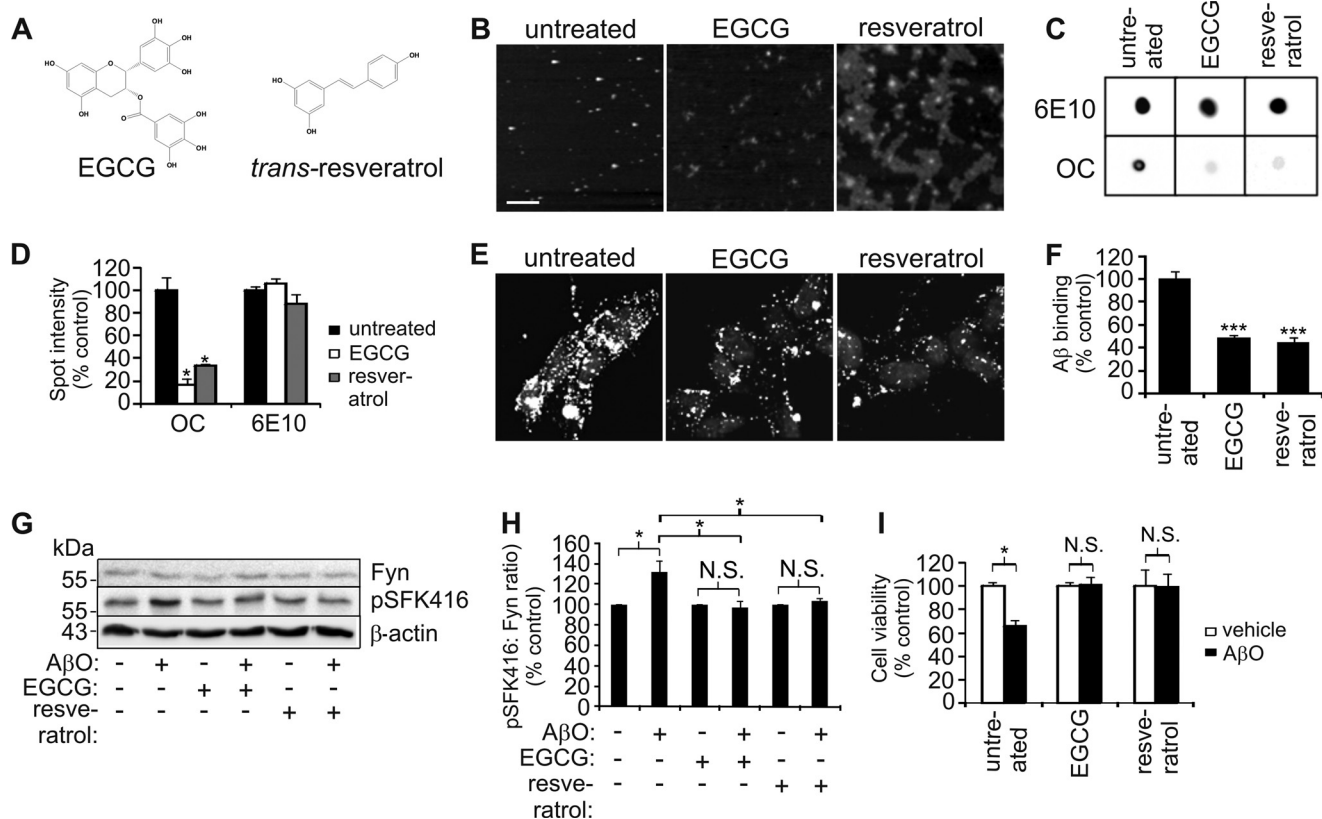
FIGURE 10. **Cellular binding, activation of Fyn kinase, and cytotoxicity of fibrillar Aβ oligomers are conformation-dependent.** *A,* structures of EGCG and *trans*-resveratrol. *B,* pre-formed AβO were incubated in the presence of EGCG (4:1 molar excess), resveratrol (10:1 molar excess), or distilled H_2O (untreated) for 24 h at room temperature and subjected to tapping mode AFM (*scale bar,* 100 nm). *C,* aliquots of the same samples from *B* (containing 1 μg of peptide) were analyzed by dot-blotting using antibodies toward Aβ (6E10) and the fibrillar conformational epitope (OC). *D,* semi-quantitative densitometry of the dot blots in *C* was performed in ImageJ ($n = 4$; *, $p = 0.021$). *E,* SH-SY5Y cells expressing PrP^C were incubated for 90 min with pre-formed Aβ oligomers (200 nM total peptide) that had been pre-treated in the presence or absence of EGCG or resveratrol for 24 h. Fluorescence microscopy was used to detect biotin-Aβ oligomer/FITC-streptavidin conjugates bound to the cells (*scale bar,* 5 μm). *F,* quantitation of Aβ oligomer binding to cells was performed using ImageJ ($n = 60$ for each condition; ***, $p < 0.001$). *G,* NB7 cells were incubated for 20 min at 37 °C with pre-formed Aβ oligomers (500 nM total peptide) that had been pre-treated in the presence or absence of EGCG or resveratrol for 24 h, relative to vehicle controls. Lysates were prepared and immunoblotted for Fyn, pSFK416, and β-actin. *H,* quantification of immunoblots for the amount of phospho-SFK normalized to Fyn kinase ($n = 6$; *, $p < 0.05$; *N.S.*, not significant). *I,* cytotoxicity of the remodeled Aβ oligomers was measured using the Multi-Tox Fluor™ multiplex cytotoxicity assay. SH-SY5Y cells expressing PrP^C were incubated for 5 h at 37 °C in the presence of AβO (500 nM total peptide) that had been pre-treated in the presence or absence of EGCG or resveratrol for 24 h, relative to vehicle controls ($n = 4$; *, $p = 0.021$; *N.S.*, not significant).

cantly reduced binding to, and were nontoxic toward, PrP^C-expressing cells. To our knowledge, this is the first demonstration that the binding of amyloid oligomers to a specific cellular receptor (PrP^C) can be prevented by remodeling the oligomer conformation. Our results demonstrate that the conformation of fibrillar Aβ oligomers is a critical determinant of their PrP^C-mediated binding and subsequent toxicity (Fig. 11*B*) and adds further weight to the proposition that disrupting the conformation of Aβ oligomers is a potential therapeutic approach for AD (70). It should be noted that the relatively high concentrations of EGCG and resveratrol used in this study are unlikely to be therapeutically attainable, especially in the brain, but lower levels may still be capable of remodeling oligomers sufficiently to disrupt their binding to PrP^C.

We have focused our attention on the interaction of fibrillar Aβ oligomers with PrP^C, as these oligomers most closely correlate with AD (32). Although fibrils have been reported not to bind to PrP^C (11, 14), our data do not rule out the possibility of other Aβ oligomers binding to PrP^C. It has been reported that various β-sheet-rich structures bind to PrP^C, including Aβ oligomers and short synthetic peptides (21). In this case, the

A11 antibody, which recognizes pre-fibrillar oligomers, was found to block the toxic signaling of Aβ oligomers through PrP^C suggesting that pre-fibrillar Aβ oligomers may also exert toxicity in a PrP^C-dependent manner. However, it should be noted that the A11 antibody has previously been shown to recognize a cytosolic form of PrP^C (71), raising the possibility that its direct binding to PrP^C may have prevented oligomer binding and the subsequent toxicity.

Our data demonstrating the importance of oligomer conformation upon biological activity, underline the importance of using well defined Aβ oligomer preparations and potentially explain the discrepancies in results showing a lack of PrP^C-dependence of Aβ oligomer toxicity, as different studies have employed distinct, often poorly characterized Aβ oligomer preparations or unnatural APP constructs which may not lead to the generation of biologically relevant Aβ oligomers (19, 20, 22).

In conclusion, our data show that the cytotoxicity of the fibrillar Aβ oligomers following their binding to PrP^C requires both the integrity of lipid rafts and the transmembrane LRP1. Also, the toxicity of fibrillar Aβ oligomers can be prevented by
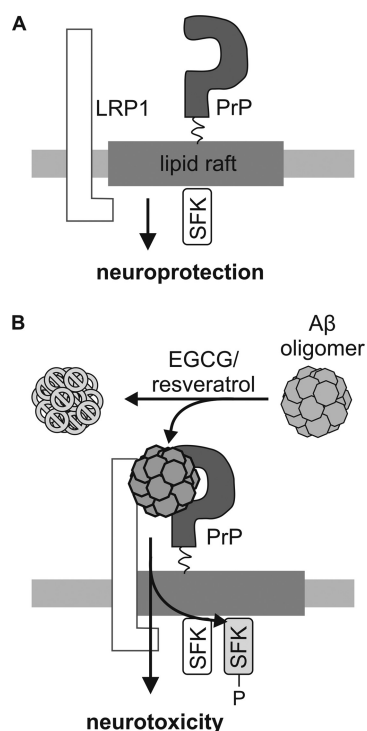
FIGURE 11. **Putative model of fibrillar Aβ oligomers binding to PrP^C in lipid rafts.** *A,* in the healthy brain, PrP^C is involved in neuroprotective signaling (72). *B,* in AD, fibrillar Aβ oligomers bind to PrP^C and the transmembrane LRP1, promoting their clustering in cholesterol-rich lipid rafts, activation of Fyn kinase, and neurotoxicity. Remodeling the conformation of the oligomers using EGCG or resveratrol prevents their PrP^C-dependent binding and toxicity.

natural, small molecules such as EGCG and resveratrol which remodel the fibrillar Aβ oligomer conformation and reduce PrP^C-mediated binding. These data identify novel molecular and cellular mechanisms that may be therapeutic targets to prevent the neurotoxicity of Aβ oligomers in AD.

REFERENCES

1. Mount, C., and Downton, C. (2006) Alzheimer disease: progress or profit? *Nat. Med.* **12,** 780–784
2. Wimo, A., and Prince, M. (2010) *World Alzheimer Report 2010: The Global Economic Impact of Dementia,* Alzheimer's Disease International, London
3. Citron, M. (2010) Alzheimer's disease: strategies for disease modification. *Nat. Rev. Drug Discov.* **9,** 387–398
4. Hardy, J. (2009) The amyloid hypothesis for Alzheimer's disease: a critical reappraisal. *J. Neurochem.* **110,** 1129–1134
5. Lue, L. F., Kuo, Y. M., Roher, A. E., Brachova, L., Shen, Y., Sue, L., Beach, T., Kurth, J. H., Rydel, R. E., and Rogers, J. (1999) Soluble amyloid β peptide concentration as a predictor of synaptic change in Alzheimer's disease. *Am. J. Pathol.* **155,** 853–862

6. Lambert, M. P., Barlow, A. K., Chromy, B. A., Edwards, C., Freed, R., Liosatos, M., Morgan, T. E., Rozovsky, I., Trommer, B., Viola, K. L., Wals, P., Zhang, C., Finch, C. E., Krafft, G. A., and Klein, W. L. (1998) Diffusible, nonfibrillar ligands derived from Aβ1–42 are potent central nervous system neurotoxins. *Proc. Natl. Acad. Sci. U.S.A.* **95,** 6448–6453
7. Lesné, S., Koh, M. T., Kotilinek, L., Kayed, R., Glabe, C. G., Yang, A., Gallagher, M., and Ashe, K. H. (2006) A specific amyloid-β protein assembly in the brain impairs memory. *Nature* **440,** 352–357
8. Walsh, D. M., Klyubin, I., Fadeeva, J. V., Cullen, W. K., Anwyl, R., Wolfe, M. S., Rowan, M. J., and Selkoe, D. J. (2002) Naturally secreted oligomers of amyloid β protein potently inhibit hippocampal long-term potentiation *in vivo. Nature* **416,** 535–539
9. Shankar, G. M., Li, S., Mehta, T. H., Garcia-Munoz, A., Shepardson, N. E., Smith, I., Brett, F. M., Farrell, M. A., Rowan, M. J., Lemere, C. A., Regan, C. M., Walsh, D. M., Sabatini, B. L., and Selkoe, D. J. (2008) Amyloid-β protein dimers isolated directly from Alzheimer's brains impair synaptic plasticity and memory. *Nat. Med.* **14,** 837–842
10. Gimbel, D. A., Nygaard, H. B., Coffey, E. E., Gunther, E. C., Laurén, J., Gimbel, Z. A., and Strittmatter, S. M. (2010) Memory impairment in transgenic Alzheimer mice requires cellular prion protein. *J. Neurosci.* **30,** 6367–6374
11. Laurén, J., Gimbel, D. A., Nygaard, H. B., Gilbert, J. W., and Strittmatter, S. M. (2009) Cellular prion protein mediates impairment of synaptic plasticity by amyloid-β oligomers. *Nature* **457,** 1128–1132
12. Prusiner, S. B. (1998) Prions. *Proc. Natl. Acad. Sci. U.S.A.* **95,** 13363–13383
13. Taylor, D. R., and Hooper, N. M. (2006) The prion protein and lipid rafts. *Mol. Membr. Biol.* **23,** 89–99
14. Chen, S., Yadav, S. P., and Surewicz, W. K. (2010) Interaction between human prion protein and amyloid-β (Aβ) oligomers. *J. Biol. Chem.* **285,** 26377–26383
15. Chung, E., Ji, Y., Sun, Y., Kascsak, R. J., Kascsak, R. B., Mehta, P. D., Strittmatter, S. M., and Wisniewski, T. (2010) Anti-PrPC monoclonal antibody infusion as a novel treatment for cognitive deficits in an Alzheimer's disease model mouse. *BMC Neurosci.* **11,** 130
16. Barry, A. E., Klyubin, I., Mc Donald, J. M., Mably, A. J., Farrell, M. A., Scott, M., Walsh, D. M., and Rowan, M. J. (2011) Alzheimer's disease brain-derived amyloid-β-mediated inhibition of LTP *in vivo* is prevented by immunotargeting cellular prion protein. *J. Neurosci.* **31,** 7259–7263
17. Freir, D. B., Nicoll, A. J., Klyubin, I., Panico, S., Mc Donald, J. M., Risse, E., Asante, E. A., Farrow, M. A., Sessions, R. B., Saibil, H. R., Clarke, A. R., Rowan, M. J., Walsh, D. M., and Collinge, J. (2011) Interaction between prion protein and toxic amyloid β assemblies can be therapeutically targeted at multiple sites. *Nat. Commun.* **2,** 336–345
18. Bate, C., and Williams, A. (2011) Amyloid-β-induced synapse damage is mediated via cross-linkage of cellular prion proteins. *J. Biol. Chem.* **286,** 37955–37963
19. Balducci, C., Beeg, M., Stravalaci, M., Bastone, A., Sclip, A., Biasini, E., Tapella, L., Colombo, L., Manzoni, C., Borsello, T., Chiesa, R., Gobbi, M., Salmona, M., and Forloni, G. (2010) Synthetic amyloid-β oligomers impair long-term memory independently of cellular prion protein. *Proc. Natl. Acad. Sci. U.S.A.* **107,** 2295–2300
20. Calella, A. M., Farinelli, M., Nuvolone, M., Mirante, O., Moos, R., Falsig, J., Mansuy, I. M., and Aguzzi, A. (2010) Prion protein and Aβ-related synaptic toxicity impairment. *EMBO Mol. Med.* **2,** 306–314
21. Resenberger, U. K., Harmeier, A., Woerner, A. C., Goodman, J. L., Müller, V., Krishnan, R., Vabulas, R. M., Kretzschmar, H. A., Lindquist, S., Hartl, F. U., Multhaup, G., Winklhofer, K. F., and Tatzelt, J. (2011) The cellular prion protein mediates neurotoxic signalling of β-sheet-rich conformers independent of prion replication. *EMBO J.* **30,** 2057–2070
22. Kessels, H. W., Nguyen, L. N., Nabavi, S., and Malinow, R. (2010) The prion protein as a receptor for amyloid-β. *Nature* **466,** E3–4
23. Vardy, E. R., Catto, A. J., and Hooper, N. M. (2005) Proteolytic mechanisms in amyloid-β metabolism: therapeutic implications for Alzheimer's disease. *Trends Mol. Med.* **11,** 464–472
24. Parkin, E. T., Watt, N. T., Hussain, I., Eckman, E. A., Eckman, C. B., Manson, J. C., Baybutt, H. N., Turner, A. J., and Hooper, N. M. (2007) Cellular prion protein regulates β-secretase cleavage of the Alzheimer's amyloid precursor protein. *Proc. Natl. Acad. Sci. U.S.A.* **104,** 11062–11067

25. Griffiths, H. H., Whitehouse, I. J., Baybutt, H., Brown, D., Kellett, K. A., Jackson, C. D., Turner, A. J., Piccardo, P., Manson, J. C., and Hooper, N. M. (2011) Prion protein interacts with BACE1 protein and differentially regulates its activity toward wild type and Swedish mutant amyloid precursor protein. *J. Biol. Chem.* **286,** 33489–33500

26. Kellett, K. A., and Hooper, N. M. (2009) Prion protein and Alzheimer disease. *Prion* **3,** 190–194

27. Walsh, D. M., and Selkoe, D. J. (2007) Aβ oligomers–a decade of discovery. *J. Neurochem.* **101,** 1172–1184

28. Glabe, C. G. (2008) Structural classification of toxic amyloid oligomers. *J. Biol. Chem.* **283,** 29639–29643

29. Kayed, R., Head, E., Sarsoza, F., Saing, T., Cotman, C. W., Necula, M., Margol, L., Wu, J., Breydo, L., Thompson, J. L., Rasool, S., Gurlo, T., Butler, P., and Glabe, C. G. (2007) Fibril-specific, conformation-dependent antibodies recognize a generic epitope common to amyloid fibrils and fibrillar oligomers that is absent in prefibrillar oligomers. *Mol. Neurodegener.* **2,** 18–29

30. Kayed, R., and Glabe, C. G. (2006) Conformation-dependent anti-amyloid oligomer antibodies. *Methods Enzymol.* **413,** 326–344

31. Kayed, R., Pensalfini, A., Margol, L., Sokolov, Y., Sarsoza, F., Head, E., Hall, J., and Glabe, C. (2009) Annular protofibrils are a structurally and functionally distinct type of amyloid oligomer. *J. Biol. Chem.* **284,** 4230–4237

32. Tomic, J. L., Pensalfini, A., Head, E., and Glabe, C. G. (2009) Soluble fibrillar oligomer levels are elevated in Alzheimer's disease brain and correlate with cognitive dysfunction. *Neurobiol. Dis.* **35,** 352–358

33. Bieschke, J., Russ, J., Friedrich, R. P., Ehrnhoefer, D. E., Wobst, H., Neugebauer, K., and Wanker, E. E. (2010) EGCG remodels mature α-synuclein and amyloid-β fibrils and reduces cellular toxicity. *Proc. Natl. Acad. Sci. U.S.A.* **107,** 7710–7715

34. Ladiwala, A. R., Lin, J. C., Bale, S. S., Marcelino-Cruz, A. M., Bhattacharya, M., Dordick, J. S., and Tessier, P. M. (2010) Resveratrol selectively remodels soluble oligomers and fibrils of amyloid Aβ into off-pathway conformers. *J. Biol. Chem.* **285,** 24228–24237

35. Ehrnhoefer, D. E., Bieschke, J., Boeddrich, A., Herbst, M., Masino, L., Lurz, R., Engemann, S., Pastore, A., and Wanker, E. E. (2008) EGCG redirects amyloidogenic polypeptides into unstructured, off-pathway oligomers. *Nat. Struct. Mol. Biol.* **15,** 558–566

36. Perera, W. S., and Hooper, N. M. (2001) Ablation of the metal ion-induced endocytosis of the prion protein by disease-associated mutation of the octarepeat region. *Curr. Biol.* **11,** 519–523

37. Rees, S., Coote, J., Stables, J., Goodson, S., Harris, S., and Lee, M. G. (1996) Bicistronic vector for the creation of stable mammalian cell lines that predisposes all antibiotic-resistant cells to express recombinant protein. *BioTechniques* **20,** 102–104

38. Watt, N. T., Taylor, D. R., Kerrigan, T. L., Griffiths, H. H., Rushworth, J. V., Whitehouse, I. J., and Hooper, N. M. (2012) Prion protein facilitates uptake of zinc into neuronal cells. *Nat. Commun.* **3,** 1134

39. Chromy, B. A., Nowak, R. J., Lambert, M. P., Viola, K. L., Chang, L., Velasco, P. T., Jones, B. W., Fernandez, S. J., Lacor, P. N., Horowitz, P., Finch, C. E., Krafft, G. A., and Klein, W. L. (2003) Self-assembly of Aβ(1–42) into globular neurotoxins. *Biochemistry* **42,** 12749–12760

40. Taylor, D. R., Watt, N. T., Perera, W. S., and Hooper, N. M. (2005) Assigning functions to distinct regions of the N terminus of the prion protein that are involved in its copper-stimulated, clathrin-dependent endocytosis. *J. Cell Sci.* **118,** 5141–5153

41. Brouillette, J., Caillierez, R., Zommer, N., Alves-Pires, C., Benilova, I., Blum, D., De Strooper, B., and Buée, L. (2012) Neurotoxicity and memory deficits induced by soluble low-molecular-weight amyloid-β1–42 oligomers are revealed *in vivo* by using a novel animal model. *J. Neurosci.* **32,** 7852–7861

42. Kudo, W., Lee, H. P., Zou, W. Q., Wang, X., Perry, G., Zhu, X., Smith, M. A., Petersen, R. B., and Lee, H. G. (2012) Cellular prion protein is essential for oligomeric amyloid-β-induced neuronal cell death. *Hum. Mol. Gen.* **21,** 1138–1144

43. Paitel, E., Alves da Costa, C., Vilette, D., Grassi, J., and Checler, F. (2002) Overexpression of PrPc triggers caspase 3 activation: potentiation by proteasome inhibitors and blockade by anti-PrP antibodies. *J. Neurochem.* **83,** 1208–1214

44. Chin, J., Palop, J. J., Puoliväli, J., Massaro, C., Bien-Ly, N., Gerstein, H., Scearce-Levie, K., Masliah, E., and Mucke, L. (2005) Fyn kinase induces synaptic and cognitive impairments in a transgenic mouse model of Alzheimer's disease. *J. Neurosci.* **25,** 9694–9703

45. Mouillet-Richard, S., Ermonval, M., Chebassier, C., Laplanche, J. L., Lehmann, S., Launay, J. M., and Kellermann, O. (2000) Signal transduction through prion protein. *Science* **289,** 1925–1928

46. Um, J. W., Nygaard, H. B., Heiss, J. K., Kostylev, M. A., Stagi, M., Vortmeyer, A., Wisniewski, T., Gunther, E. C., and Strittmatter, S. M. (2012) Alzheimer amyloid-β oligomer bound to postsynaptic prion protein activates Fyn to impair neurons. *Nat. Neurosci.* **15,** 1227–1235

47. Williamson, R., Usardi, A., Hanger, D. P., and Anderton, B. H. (2008) Membrane-bound β-amyloid oligomers are recruited into lipid rafts by a Fyn-dependent mechanism. *FASEB J.* **22,** 1552–1559

48. Taylor, D. R., and Hooper, N. M. (2007) The low-density lipoprotein receptor-related protein 1 (LRP1) mediates the endocytosis of the cellular prion protein. *Biochem. J.* **402,** 17–23

49. Parkyn, C. J., Vermeulen, E. G., Mootoosamy, R. C., Sunyach, C., Jacobsen, C., Oxvig, C., Moestrup, S., Liu, Q., Bu, G., Jen, A., and Morris, R. J. (2008) LRP1 controls biosynthetic and endocytic trafficking of neuronal prion protein. *J. Cell Sci.* **121,** 773–783

50. Kanekiyo, T., and Bu, G. (2009) Receptor-associated protein interacts with amyloid-β peptide and promotes its cellular uptake. *J. Biol. Chem.* **284,** 33352–33359

51. Rambold, A. S., Miesbauer, M., Olschewski, D., Seidel, R., Riemer, C., Smale, L., Brumm, L., Levy, M., Gazit, E., Oesterhelt, D., Baier, M., Becker, C. F., Engelhard, M., Winklhofer, K. F., and Tatzelt, J. (2008) Green tea extracts interfere with the stress-protective activity of PrP and the formation of PrP. *J. Neurochem.* **107,** 218–229

52. Salès, N., Rodolfo, K., Hässig, R., Faucheux, B., Di Giamberardino, L., and Moya, K. L. (1998) Cellular prion protein localization in rodent and primate brain. *Eur. J. Neurosci.* **10,** 2464–2471

53. Liu, T., Zwingman, T., Li, R., Pan, T., Wong, B. S., Petersen, R. B., Gambetti, P., Herrup, K., and Sy, M. S. (2001) Differential expression of cellular prion protein in mouse brain as detected with multiple anti-PrP monoclonal antibodies. *Brain Res.* **896,** 118–129

54. Haass, C., and Mandelkow, E. (2010) Fynτ-amyloid: a toxic triad. *Cell* **142,** 356–358

55. Roberson, E. D., Halabisky, B., Yoo, J. W., Yao, J., Chin, J., Yan, F., Wu, T., Hamto, P., Devidze, N., Yu, G.-Q., Palop, J. J., Noebels, J. L., and Mucke, L. (2011) Amyloid-β/Fyn-induced synaptic, network, and cognitive impairments depend on Tau levels in multiple mouse models of Alzheimer's disease. *J. Neurosci.* **31,** 700–711

56. Lewis, V., and Hooper, N. M. (2011) The role of lipid rafts in prion protein biology. *Front. Biosci.* **16,** 151–168

57. Caetano, F. A., Lopes, M. H., Hajj, G. N., Machado, C. F., Pinto Arantes, C., Magalhães, A. C., Vieira Mde, P., Américo, T. A., Massensini, A. R., Priola, S. A., Vorberg, I., Gomez, M. V., Linden, R., Prado, V. F., Martins, V. R., and Prado, M. A. (2008) Endocytosis of prion protein is required for ERK1/2 signaling induced by stress-inducible protein 1. *J. Neurosci.* **28,** 6691–6702

58. Chafekar, S. M., Baas, F., and Scheper, W. (2008) Oligomer-specific Aβ toxicity in cell models is mediated by selective uptake. *Biochim. Biophys. Acta* **1782,** 523–531

59. Caetano, F. A., Beraldo, F. H., Hajj, G. N., Guimaraes, A. L., Jürgensen, S., Wasilewska-Sampaio, A. P., Hirata, P. H., Souza, I., Machado, C. F., Wong, D. Y., De Felice, F. G., Ferreira, S. T., Prado, V. F., Rylett, R. J., Martins, V. R., and Prado, M. A. (2011) Amyloid-β oligomers increase the localization of prion protein at the cell surface. *J. Neurochem.* **117,** 538–553

60. Nykjaer, A., and Willnow, T. E. (2002) The low-density lipoprotein receptor gene family: a cellular Swiss army knife? *Trends Cell Biol.* **12,** 273–280

61. Kanekiyo, T., Zhang, J., Liu, Q., Liu, C.-C., Zhang, L., and Bu, G. (2011) Heparan sulphate proteoglycan and the low-density lipoprotein receptor-related protein 1 constitute major pathways for neuronal amyloid-β uptake. *J. Neurosci.* **31,** 1644–1651

62. Fuentealba, R. A., Liu, Q., Zhang, J., Kanekiyo, T., Hu, X., Lee, J. M., LaDu, M. J., and Bu, G. (2010) Low-density lipoprotein receptor-related protein 1 (LRP1) mediates neuronal Aβ42 uptake and lysosomal trafficking. *PLoS*

One **5,** e11884

63. Wu, L., and Gonias, S. L. (2005) The low-density lipoprotein receptor-related protein-1 associates transiently with lipid rafts. *J. Cell. Biochem.* **96,** 1021–1033

64. Cisse, M., and Mucke, L. (2009) Alzheimer's disease: A prion protein connection. *Nature* **457,** 1090–1091

65. Linden, R., Martins, V. R., Prado, M. A., Cammarota, M., Izquierdo, I., and Brentani, R. R. (2008) Physiology of the prion protein. *Physiol. Rev.* **88,** 673–728

66. Renner, M., Lacor, P. N., Velasco, P. T., Xu, J., Contractor, A., Klein, W. L., and Triller, A. (2010) Deleterious effects of amyloid β oligomers acting as an extracellular scaffold for mGluR5. *Neuron* **66,** 739–754

67. Pflanzner, T., Petsch, B., André-Dohmen, B., Müller-Schiffmann, A., Tschickardt, S., Weggen, S., Stitz, L., Korth, C., and Pietrzik, C. U. (2012) Cellular prion protein participates in amyloid-β transcytosis across the blood-brain barrier. *J. Cereb. Blood Flow Metab.* **32,** 628–632

68. Zeng, F., Watt, N. T., Walmsley, A. R., and Hooper, N. M. (2003) Tethering the N terminus of the prion protein compromises the cellular response to oxidative stress. *J. Neurochem.* **84,** 480–490

69. Dupiereux, I., Falisse-Poirrier, N., Zorzi, W., Watt, N. T., Thellin, O., Zorzi, D., Pierard, O., Hooper, N. M., Heinen, E., and Elmoualij, B. (2008) Protective effect of prion protein via the N-terminal region in mediating a protective effect on paraquat-induced oxidative injury in neuronal cells. *J. Neurosci. Res.* **86,** 653–659

70. Broersen, K., Rousseau, F., and Schymkowitz, J. (2010) The culprit behind amyloid β peptide related neurotoxicity in Alzheimer's disease: oligomer size or conformation? *Alzheimers Res. Ther.* **2,** 12–26

71. Wang, X., Bowers, S. L., Wang, F., Pu, X. A., Nelson, R. J., and Ma, J. (2009) Cytoplasmic prion protein induces forebrain neurotoxicity. *Biochim. Biophys. Acta* **1792,** 555–563

72. Roucou, X., and LeBlanc, A. C. (2005) Cellular prion protein neuroprotective function: implications in prion diseases. *J. Mol. Med.* **83,** 3–11